

## ERROR ANALYSIS FOR POD APPROXIMATIONS OF INFINITE HORIZON PROBLEMS VIA THE DYNAMIC PROGRAMMING APPROACH\*

A. ALLA<sup>†</sup>, M. FALCONE<sup>‡</sup>, AND S. VOLKWEIN<sup>§</sup>

**Abstract.** In this paper infinite horizon optimal control problems for nonlinear high-dimensional dynamical systems are studied. Nonlinear feedback laws can be computed via the value function characterized as the unique viscosity solution to the corresponding Hamilton–Jacobi–Bellman (HJB) equation which stems from the dynamic programming approach. However, the bottleneck is mainly due to the *curse of dimensionality*, and HJB equations are solvable only in a relatively small dimension. Therefore, a reduced-order model is derived for the dynamical system, using the method of proper orthogonal decomposition (POD). The resulting errors in the HJB equations are estimated by an a priori error analysis, which is utilized in the numerical approximation to ensure a desired accuracy for the POD method. Numerical experiments illustrates the theoretical findings.

**Key words.** optimal control, nonlinear dynamical systems, Hamilton–Jacobi–Bellman equation, proper orthogonal decomposition, error analysis

**AMS subject classifications.** 35K20, 49L20, 49L25, 49J20, 65N99

**DOI.** 10.1137/15M1039596

**1. Introduction.** The dynamic programming approach to the solution of optimal control problems driven by dynamical systems in  $\mathbb{R}^n$  offers a nice framework for the approximation of feedback laws and optimal trajectories. It suffers from the bottleneck of the computation of the value function since this requires the approximation of a nonlinear partial differential equation (PDE) in dimension  $n$ . This is a very challenging problem in high dimensions due to the huge amount of memory allocation necessary to work on a grid and to the low regularity properties of the value function (which is typically only Lipschitz-continuous for regular dynamics and running costs). Despite the number of theoretical results established for many classical control problems via the dynamic programming approach (see, e.g., the monographs by Bardi and Capuzzo-Dolcetta [9] on deterministic control problems, and by Fleming and Soner [22] on stochastic control problems), this has always been the main obstacle to applying this nowadays rather complete theory to real applications. The “curse of dimensionality” has been mitigated via domain decomposition techniques and the development of rather efficient numerical methods, but it is still a big obstacle. Although a detailed description of these contributions goes beyond the scope of this paper, we want to mention [21] for a domain decomposition method with overlap between the subdomains, and [13] for similar results without overlap. It is important to note that in these papers the method is applied to subdomains with a rather simple geometry (see the book by Quarteroni and Valli [35] for a general introduction to this technique) in order to apply transmission conditions at the boundaries. More recently

---

\*Received by the editors September 14, 2015; accepted for publication (in revised form) July 26, 2017; published electronically October 3, 2017.

<http://www.siam.org/journals/sicon/55-5/M103959.html>

<sup>†</sup>Corresponding author. Department of Scientific Computing, Florida State University, Tallahassee, FL 32306 (aalla@fsu.edu).

<sup>‡</sup>Dipartimento di Matematica, SAPIENZA - Università di Roma, P.le Aldo Moro 2, I-00185 Rome, Italy (falcone@mat.uniroma1.it).

<sup>§</sup>Department of Mathematics and Statistics, Universität Konstanz, Universitätsstraße 10, D-78457 Konstanz, Germany (Stefan.Volkwein@uni-konstanz.de).

another way to decompose the problem has been proposed by Navasca and Krener [34], who have used a patchy decomposition based on the Al'brekht method. Later, in the paper [12], the patchy idea was implemented by taking into account an approximation of the underlying optimal dynamics to obtain subdomains which are almost invariant with respect to the optimal dynamics; clearly in this case the geometry of the subdomains can be rather complex, but the transmission conditions at the internal boundaries can be eliminated, saving on the overall complexity of the algorithm. In general, domain decomposition methods reduce a huge problem into subproblems of manageable size and allow one to mitigate storage limitations by distributing the computation over several processors. However, the approximation schemes used in every subdomain are rather standard. Another improvement can be obtained using efficient acceleration methods for the computation of the value function in every subdomain. To this end one can use fast marching methods [37, 38] and fast sweeping methods [42] for specific classes of Hamilton–Jacobi equations. In the framework of optimal control problems an efficient acceleration technique based on the coupling between value and policy iterations has been recently proposed and studied by Alla, Falcone, and Kalise in [2]. Finally, we should mention that the interested reader can find in [19] a number of successful applications to optimal control problems and games in rather low dimension.

In parallel to these results, several model reduction techniques have been developed to deal with high-dimensional dynamics in a rather economical way. These techniques are really necessary when dealing with optimal control problems governed by PDEs. Despite the vast literature concerning the analysis and numerical approximation of optimal control problems for PDEs, the number of works devoted to the synthesis of feedback controllers is rather small. In this direction, the dynamic programming principle (DPP) is a powerful technique which has been applied mainly to linear dynamics, quadratic cost functions, and unbounded control space, the so-called linear quadratic regulator (LQR) control problem. For this problem an explicit feedback controller can be computed by means of the solution of an algebraic Riccati equation. However, if the underlying structural assumptions are removed, the feedback control has to be obtained via approximation of a Hamilton–Jacobi–Bellman (HJB) equation defined over the state space of the system dynamics. As we mentioned, this is a major bottleneck for the application of DPP-based techniques in the optimal control of PDEs, as the natural approach for this class of control problems is to consider a semidiscretization (in space) via finite elements or finite differences of the abstract governing equations, leading to an inherently high-dimensional state space. However, in the last years several steps have been made to obtain reduced-order models for complicated dynamics, and by the application of these techniques it is now possible to have a reasonable approximation of large-scale dynamics using a rather small number of basis functions. This can open the way to the DPP approach in high-dimensional systems.

Reduced-order models are used in PDE-constrained optimization in various ways; see, e.g., [11, 25, 28, 36] for a survey. However, the main stream for the optimal control of PDEs is still related to open-loop controls based on the Pontryagin maximum principle. (An extensive presentation of this classical approach can be found in the monograph [27, 43].) We refer the reader to [3, 5, 7, 31, 32, 33], where it has been observed that models of reduced order can play an important and very useful role in the implementation of feedback laws. To the best of our knowledge, a priori error analysis for the approximation of the value function was not derived. More recently, the proper orthogonal decomposition (POD) has been proposed for PDE control problems in or-

der to reduce the dynamics to a small number of state variables via a careful selection of the snapshots. This technique, coupled with the dynamic programming approach, has been developed mainly for linear equations starting from the heat equation, where one can take advantage of the regularity of the solutions to reduce the dimension [5], and then attacking more difficult problems such as the advection-diffusion [1, 4, 29], Burgers’s [31, 32], and Navier–Stokes [3] equations. In [30] the authors apply HJB equations to the control of a PDE, although they are not using model reduction.

The aim of this paper is to study the interplay between reduced-order dynamics, the associated dynamic programming equation, the resulting feedback controller, and its performance over the high-dimensional system. In our analysis we will derive some a priori error estimates which take into account the time and space discretization parameters  $\Delta t$  and  $\Delta x$  as well as the dimension  $\ell$  of the POD basis functions used for the reduced model. Clearly other types of approximations, e.g., sparse grids [23], and different model reduction techniques can be applied (as in [6]), but the analysis of these couplings to obtain analogous error estimates goes beyond the scope of this paper.

The paper is organized as follows. In section 2 we recall some basic facts about the approximation of the infinite horizon problem via the dynamic programming approach. Section 3 is devoted to briefly presenting the POD technique and the basic ideas behind the construction of the reduced model. In section 4 we present the main results and our a priori estimates for the numerical approximation of the reduced model. These a priori estimates have also been used in the construction of the algorithm which is described in detail in section 5. Some numerical tests are presented and analyzed in section 6, and finally we draw some conclusions in section 7.

**2. Optimal control problem.** In this section we will recall the dynamic programming approach and its numerical approximation for the solution of infinite horizon control problems.

**2.1. The infinite horizon problem.** For given nonlinear mapping  $f : \mathbb{R}^n \times \mathbb{R}^m \rightarrow \mathbb{R}^n$  and initial condition  $y_0 \in \mathbb{R}^n$  let us consider the controlled nonlinear dynamical systems

$$(2.1) \quad \dot{y}(t) = f(y(t), u(t)) \in \mathbb{R}^n \quad \text{for } t > 0, \quad y(0) = y_0 \in \mathbb{R}^n,$$

together with the infinite horizon cost functional

$$(2.2) \quad J(y, u) = \int_0^\infty g(y(t), u(t)) e^{-\lambda t} dt.$$

In (2.2) we assume that  $\lambda > 0$  is a given weighting parameter and that  $g$  maps  $\mathbb{R}^n \times \mathbb{R}^m$  to  $\mathbb{R}$ . The set of admissible controls has the form

$$\mathbb{U}_{\text{ad}} = \{u \in \mathbb{U} \mid u(t) \in U_{\text{ad}} \text{ for almost all } t \geq 0\},$$

where we set  $\mathbb{U} = L^2(0, \infty; \mathbb{R}^m)$  and  $U_{\text{ad}} \subset \mathbb{R}^m$  denotes a compact convex subset. We note that we could also choose  $\mathbb{U} = L^\infty(0, T; \mathbb{U}_{\text{ad}})$ , but working in a Hilbert space is convenient for writing gradients.

The infinite horizon problem has been chosen as a model problem to simplify the analysis and to deal with the stationary HJB equations. Although the aforementioned equations have an interest in themselves, it is also useful to investigate long-time behavior of finite horizon problems. We note that a priori error estimates

for the dynamic programming approximation of other classical control problems are also available in, e.g., [19] (for the finite horizon problem, see [20]), so the analysis in this paper gives a rather general framework which could possibly be extended to the finite horizon and other classical control problems.

Throughout our paper we suppose the following hypotheses.

ASSUMPTION 2.1.

1. *The right-hand side  $f : \mathbb{R}^n \times \mathbb{R}^m \rightarrow \mathbb{R}^n$  from (2.1) is continuous and globally Lipschitz-continuous in the first argument; i.e., there exists an  $L_f > 0$  satisfying*

$$\|f(y, u) - f(\tilde{y}, u)\|_2 \leq L_f \|y - \tilde{y}\|_2 \quad \text{for all } y, \tilde{y} \in \mathbb{R}^n \text{ and } u \in U_{\text{ad}}.$$

*Furthermore,  $\|f(y, u)\|_\infty = \max_{1 \leq i \leq n} |f_i(y, u)|$  is bounded by a constant  $M_f$  for all  $y$  that belongs to a compact set  $\bar{\Omega} \subset \mathbb{R}^n$  and  $u \in U_{\text{ad}}$  (see (2.7) for more details on  $\bar{\Omega}$ ).*

2. *The running cost  $g : \mathbb{R}^n \times \mathbb{R}^m \rightarrow \mathbb{R}^n$  is continuous and globally Lipschitz-continuous in the first argument with a Lipschitz constant  $L_g > 0$ . Moreover,  $\|g(y, u)\|_\infty \leq M_g$  for all  $(y, u) \in \bar{\Omega} \times U_{\text{ad}}$  with  $M_g > 0$ .*
3. *The semiconcavity assumptions*

$$\begin{aligned} \|f(y + \tilde{y}, u) - 2f(y, u) + f(y - \tilde{y}, u)\|_2 &\leq C_f \|\tilde{y}\|_2^2, \\ |g(y + \tilde{y}, u) - 2g(y, u) + g(y - \tilde{y}, u)| &\leq C_g \|\tilde{y}\|_2^2 \end{aligned}$$

*hold for all  $(y, \tilde{y}, u) \in \mathbb{R}^n \times \mathbb{R}^n \times U_{\text{ad}}$ .*

In (2.1) we call  $y$  the *state* and  $u$  the *control*.

Let  $M \in \mathbb{R}^{n \times n}$  denote a symmetric positive definite (mass) matrix with smallest and largest positive eigenvalues  $\lambda_{\min}$  and  $\lambda_{\max}$ , respectively. Then, we introduce the following weighted inner product in  $\mathbb{R}^n$ :

$$\langle \varphi, \tilde{\varphi} \rangle_M = \varphi^\top M \tilde{\varphi} \quad \text{for } \varphi, \tilde{\varphi} \in \mathbb{R}^n,$$

where “ $\top$ ” stands for the transpose of a given vector or matrix. By  $\|\cdot\|_M = \langle \cdot, \cdot \rangle_M^{1/2}$  we define the associated induced norm.

*Remark 2.2.* The mass matrix allows different inner products for the computation of the POD basis functions. In our numerical experiments, the mass matrix is the identity because we deal with a finite difference discretization.

Recall that we have

$$\lambda_{\min} \|\varphi\|_2^2 \leq \|\varphi\|_M^2 \leq \lambda_{\max} \|\varphi\|_2^2 \quad \text{for all } \varphi \in \mathbb{R}^n.$$

Then,  $y = y(t)$  solves (2.1) if

$$(2.3) \quad \begin{aligned} \langle \dot{y}(t) - f(y(t), u(t)), \varphi \rangle_M &= 0 \quad \text{for all } \varphi \in \mathbb{R}^n \text{ and for almost all } t > 0, \\ \langle y(0) - y_o, \varphi \rangle_M &= 0 \quad \text{for all } \varphi \in \mathbb{R}^n. \end{aligned}$$

We call (2.3) the *variational formulation* of the dynamical system. It follows from Assumption 2.1 that (2.1) has a unique solution  $y = y(u; y_o) \in \mathbb{Y} = W^{1,1}(0, \infty; \mathbb{R}^n)$  for every admissible control  $u \in U_{\text{ad}}$  and for every initial condition  $y_o \in \mathbb{R}^n$ ; see, e.g., [9, Chapter III]. Thus, we can define the reduced cost functional as follows:

$$\hat{J}(u; y_o) = J(y(u; y_o), u) \quad \text{for } u \in U_{\text{ad}} \text{ and } y_o \in \mathbb{R}^n,$$

where  $y(u; y_o)$  solves (2.1) for given control  $u$  and initial condition  $y_o$ . Then, our optimal control can be formulated as follows: for given  $y_o \in \mathbb{R}^n$  we consider

$$(\widehat{\mathbf{P}}) \quad \min_{u \in U_{ad}} \widehat{J}(u; y_o).$$

**2.2. The HJB equation and its time discretization.** We define the *value function* of the problem  $v : \mathbb{R}^n \rightarrow \mathbb{R}$  as follows:

$$v(y) = \inf \{ \widehat{J}(u; y) \mid u \in U_{ad} \} \quad \text{for } y \in \mathbb{R}^n.$$

This function gives the best value for every initial condition, given the set of admissible controls  $U_{ad}$ . It is characterized as the viscosity solution of the *HJB equation* corresponding to the infinite horizon

$$(2.4) \quad \lambda v(y) + \sup_{u \in U_{ad}} \{ -f(y, u) \cdot \nabla v(y) - g(y, u) \} = 0 \quad \text{for } y \in \mathbb{R}^n,$$

which is unique for sufficiently large  $\lambda$ , as indicated in Theorem 2.3. In order to construct the approximation scheme (as in [17]) let us consider first a time discretization where  $h$  is a strictly positive step size. A DPP for the discrete time problem holds true given the following semidiscrete scheme for (2.4):

$$(2.5) \quad v_h(y) = \min_{u \in U_{ad}} \{ (1 - \lambda h)v_h(y + hf(y, u)) + hg(y, u) \} \quad \text{for } y \in \mathbb{R}^n.$$

If Assumptions 2.1.1 and 2.1.2 and  $\lambda > L_f$  hold, the function  $v_h$  is Lipschitz-continuous and satisfies

$$(2.6) \quad |v_h(y) - v_h(\tilde{y})| \leq \frac{L_g}{\lambda - L_f} \|y - \tilde{y}\|_2 \quad \text{for all } y, \tilde{y} \in \overline{\Omega} \text{ and } h \in [0, 1/\lambda);$$

see [18, p. 473]. Let us recall the following result [17, Theorem 2.3].

**THEOREM 2.3.** *Let Assumption 2.1 and  $\lambda > \max\{L_g, L_f\}$  hold. Let  $v$  and  $v_h$  be the solutions of (2.4) and (2.5), respectively. Then, there is a constant  $C \geq 0$  satisfying*

$$\sup_{y \in \mathbb{R}^n} |v(y) - v_h(y)| \leq Ch \quad \text{for any } h \in [0, 1/\lambda),$$

where the constant  $C$  can be bounded explicitly; cf. [17, Remark 1].

**2.3. The large-scale approximation of the HJB equations.** For the numerical implementation of the approximation scheme for the above mentioned Hamilton–Jacobi equation, we have to restrict ourselves to a bounded subset of  $\mathbb{R}^n$ . Let us suppose, to simplify, that there exists a (bounded) polyhedron  $\Omega \subset \mathbb{R}^n$  such that for sufficiently small  $h > 0$

$$(2.7) \quad y + hf(y, u) \in \overline{\Omega} \quad \text{for all } y \in \overline{\Omega} \text{ and } u \in U_{ad},$$

where  $\overline{\Omega}$  denotes the closure of  $\Omega$ . In [17] a sufficient condition for (2.7) was proved; in this paper we start directly from (2.7). If assumption (2.7) is not satisfied, the method proposed below can still work for optimal control problems with state constraints under weaker assumptions; e.g., for every point  $y \in \overline{\Omega}$  there exists an admissible control  $\hat{u}(y)$  such that the vector  $f(y, \hat{u}(y))$  points strictly inward (see, e.g., [40, 41]). Test 2 in section 6 will show one of these examples. We refer the interested reader to [19]

for some hints on the implementation of these and more general boundary conditions as well as for additional references. We want to point out that the above invariance condition (2.7) is used here to simplify the problem and to avoid the introduction of state constraint boundary conditions in order to focus our attention on the a priori error estimate. Furthermore, we note that the numerical approximation proposed in this paper will be applied to the problem in reduced coordinates obtained via the POD method introduced in section 3 since the problem in  $\mathbb{R}^n$  for a large  $n$  is practically unfeasible.

From the numerical viewpoint, since we are going to use a regular simplicial mesh of the domain  $\Omega$ , we need the latter to be bounded in order to keep the complexity of the problem finite. Thus, the choice of  $\Omega$  is made for convenience, and every invariant set  $\Omega$  satisfying (2.7) will fit. Let  $\{\mathcal{S}_j\}_{j=1}^{m_s}$  be a family of simplices which defines a regular triangulation of the polyhedron  $\Omega$  (see, e.g., [24]) such that

$$(2.8) \quad \bar{\Omega} = \bigcup_{j=1}^{m_s} \mathcal{S}_j \quad \text{and} \quad k = \max_{1 \leq j \leq m_s} (\text{diam } \mathcal{S}_j).$$

Throughout this paper we assume that we have  $n_s$  vertices/nodes  $y_1, \dots, y_{n_s}$  in the triangulation. Let  $V^k$  be the space of piecewise affine functions from  $\bar{\Omega}$  to  $\mathbb{R}$  which are continuous in  $\bar{\Omega}$  having constant gradients in the interior of any simplex  $\mathcal{S}_j$  of the triangulation. Then, a fully discrete scheme for the HJB equations is given by

$$(2.9) \quad v_{hk}(y_i) = \min_{u \in U_{ad}} \{ (1 - \lambda h)v_{hk}(y_i + hf(y_i, u)) + hg(y_i, u) \}$$

for any vertex  $y_i \in \bar{\Omega}$ . Clearly, a solution to (2.5) satisfies (2.9).

Let us recall the following result (see [17, Corollary 2.4] and [18, Theorem 1.3]).

**THEOREM 2.4.** *Assume that Assumption 2.1 and (2.7) hold. Let  $v$ ,  $v_h$ , and  $v_{hk}$  be the solutions of (2.4), (2.5), and (2.9), respectively. For  $\lambda > L_f$  we obtain*

$$(2.10) \quad \|v_h - v_{hk}\|_{C(\bar{\Omega})} \leq \frac{L_f}{\lambda(\lambda - L_f)} \frac{k}{h} \quad \text{for any } h \in \left[0, \frac{1}{\lambda}\right).$$

For  $\lambda > \max\{L_f, 2L_g\}$  we have

$$(2.11) \quad \|v - v_{hk}\|_{C(\bar{\Omega})} \leq Ch + \frac{L_g}{\lambda - L_f} \frac{k}{h} \quad \text{for any } h \in \left[0, \frac{1}{\lambda}\right).$$

**COROLLARY 2.5.** *Assume that Assumption 2.1 and  $\lambda > L_f$  hold. Let  $v_{hk}$  be the solution of (2.9). Then, we have for  $h \in [0, 1/\lambda]$*

$$|v_{hk}(y) - v_{hk}(\tilde{y})| \leq C_1 \frac{k}{h} + C_2 \|y - \tilde{y}\|_2 \quad \text{for all } y, \tilde{y} \in \bar{\Omega},$$

where  $C_1 = 2L_f/(\lambda(\lambda - L_f))$  and  $C_2 = L_g/(\lambda - L_f)$ .

*Proof.* Suppose that  $v_h$  is the solution to (2.5). Then, we derive from (2.6) and (2.10) that

$$\begin{aligned} |v_{hk}(y) - v_{hk}(\tilde{y})| &\leq |v_{hk}(y) - v_h(y)| + |v_h(y) - v_h(\tilde{y})| + |v_h(\tilde{y}) - v_{hk}(\tilde{y})| \\ &\leq \frac{2L_f}{\lambda(\lambda - L_f)} \frac{k}{h} + \frac{L_g}{\lambda - L_f} \|y - \tilde{y}\|_2, \end{aligned}$$

which gives the claim. □

**3. The POD method and reduced-order modeling.** The focus of this section is the construction of surrogate models by means of the POD. Here we recall the basics of the method and apply it to optimal control problems. For more details we refer the reader to, e.g., [14, 25, 26, 39].

**3.1. POD for parametrized nonlinear dynamical systems.** For  $p \in \mathbb{N}$  let us choose different pairs  $\{(u^\nu, y^\nu_\circ)\}_{\nu=1}^p$  in  $\mathbb{U}_{\text{ad}} \times \overline{\Omega}$ . By  $y^\nu = y(u^\nu; y^\nu_\circ) \in \mathbb{Y}$ ,  $\nu = 1, \dots, p$ , we denote the solution to (2.1). We introduce the *snapshot subspace* as

$$\mathcal{V} = \text{span} \{y^\nu(t) \mid t \in [0, \infty) \text{ and } 1 \leq \nu \leq p\} \subset \mathbb{R}^n.$$

For every  $\ell \in \{1, \dots, d\}$ , with dimension  $d \leq n$ , a *POD basis of rank  $\ell$*  is defined as a solution to the minimization problem

$$(\mathbf{P}^\ell) \quad \begin{cases} \min \sum_{\nu=1}^p \int_0^\infty \left\| y^\nu(t) - \sum_{i=1}^\ell \langle y^\nu(t), \psi_i \rangle_M \psi_i \right\|_M^2 dt \\ \text{such that } \{\psi_i\}_{i=1}^\ell \subset \mathbb{R}^n \text{ and } \langle \psi_i, \psi_j \rangle_M = \delta_{ij}, \quad 1 \leq i, j \leq \ell, \end{cases}$$

where  $\delta_{ij}$  is the Kronecker symbol satisfying  $\delta_{ii} = 1$  and  $\delta_{ij} = 0$  for  $i \neq j$ . It is well known that a solution to  $(\mathbf{P}^\ell)$  is given by the solution of the eigenvalue problem

$$\mathcal{R}\psi_i = \lambda_i \psi_i \quad \text{for } \lambda_1 \geq \lambda_2 \geq \dots \geq \lambda_\ell \geq \lambda_{\ell+1} > 0$$

with the linear, bounded, symmetric integral operator  $\mathcal{R} : \mathbb{R}^n \rightarrow \mathcal{V}$ ,

$$\mathcal{R}\psi = \sum_{\nu=1}^p \int_0^\infty \langle y^\nu(t), \psi \rangle_M y^\nu(t) dt \quad \text{for } \psi \in \mathbb{R}^n.$$

If  $\{\psi_i\}_{i=1}^\ell$  is a solution to  $(\mathbf{P}^\ell)$ , we have the approximation error

$$(3.1) \quad \sum_{\nu=1}^p \int_0^\infty \left\| y^\nu(t) - \sum_{i=1}^\ell \langle y^\nu(t), \psi_i \rangle_M \psi_i \right\|_M^2 dt = \sum_{i=\ell+1}^d \lambda_i.$$

In real computations, we do not have the whole trajectory  $y(t)$  for all  $t \in [0, \infty)$ . For that purpose we choose  $T \gg 0$  sufficiently large and define a grid in  $[0, t_e]$ , where  $t_e \geq T$ , by  $0 = t_1 < t_2 < \dots < t_{n_T} = t_e$ . Let  $y_j^\nu \approx y^\nu(t_j) \in \mathbb{R}^n$  denote approximations for the introduced trajectories  $\{y_j^\nu\}_{\nu=1}^p$  at the time instance  $t_j$  for  $j = 1, \dots, n_T$ . We set  $\mathcal{V}^{n_T} = \text{span} \{y_j^\nu \mid 1 \leq j \leq n_T, 1 \leq \nu \leq p\}$  with  $d^{n_T} = \dim \mathcal{V}^{n_T} \leq \min(n, n_T p)$ . Then, for every  $\ell \in \{1, \dots, d^{n_T}\}$  we consider the minimization problem

$$(\mathbf{P}^\ell_{n_T}) \quad \begin{cases} \min \sum_{\nu=1}^p \sum_{j=1}^{n_T} \alpha_j^{n_T} \left\| y_j^\nu - \sum_{i=1}^\ell \langle y_j^\nu, \psi_i^{n_T} \rangle_M \psi_i^{n_T} \right\|_M^2 \\ \text{such that } \{\psi_i^{n_T}\}_{i=1}^\ell \subset \mathbb{R}^n \text{ and } \langle \psi_i^{n_T}, \psi_j^{n_T} \rangle_M = \delta_{ij}, \quad 1 \leq i, j \leq \ell, \end{cases}$$

instead of  $(\mathbf{P}^\ell)$ . In  $(\mathbf{P}^\ell_{n_T})$  the  $\alpha_j$ 's stand for the trapezoidal weights

$$\alpha_1^{n_T} = \frac{t_2 - t_1}{2}, \quad \alpha_j^{n_T} = \frac{t_j - t_{j-1}}{2} \text{ for } 2 \leq j \leq n_T - 1, \quad \alpha_{n_T}^{n_T} = \frac{t_{n_T} - t_{n_T-1}}{2}.$$

The solution to  $(\mathbf{P}^\ell_{n_T})$  is given by the solution to the eigenvalue problem

$$\mathcal{R}^{n_T} \psi_i^{n_T} = \lambda_i^{n_T} \psi_i^{n_T} \quad \text{for } \lambda_1^{n_T} \geq \lambda_2^{n_T} \geq \dots \geq \lambda_\ell^{n_T} \geq \lambda_{d^{n_T}}^{n_T} > 0$$

with the linear, bounded, symmetric, and nonnegative operator

$$\mathcal{R}^{n_T} \psi = \sum_{\nu=1}^p \sum_{j=1}^{n_T} \alpha_j^{n_T} \langle y_j^\nu, \psi \rangle_M y_j^\nu \quad \text{for } \psi \in \mathbb{R}^n.$$

Analogous to (3.1), a solution to  $(\mathbf{P}_{n_T}^\ell)$  satisfies

$$(3.2) \quad \sum_{\nu=1}^p \sum_{j=1}^{n_T} \alpha_j^{n_T} \left\| y_j^\nu - \sum_{i=1}^{\ell} \langle y_j^\nu, \psi_i^{n_T} \rangle_M \psi_i^{n_T} \right\|_M^2 = \sum_{i=\ell+1}^{d^{n_T}} \lambda_i^{n_T}.$$

**3.2. Reduced-order modelling for the state equation.** We introduce the POD coefficient matrix

$$\Psi = [\psi_1 \mid \dots \mid \psi_\ell] \in \mathbb{R}^{n \times \ell}$$

and the subspace  $V^\ell = \text{span}\{\psi_1, \dots, \psi_\ell\} \subset \mathbb{R}^n$ . In particular, the matrix  $M^\ell = \Psi^\top M \Psi \in \mathbb{R}^{\ell \times \ell}$  is the identity matrix. The reduced-order model for (2.3) is derived as follows: we replace the vector  $y(t) \in \mathbb{R}^n$  by its POD approximation  $\Psi y^\ell(t) \in \mathbb{R}^n$  with the unknown time dependent coefficients  $y^\ell(t) \in \mathbb{R}^\ell$  and choose  $\varphi = \psi_i$  for  $i = 1, \dots, \ell$ . It follows that

$$(3.3) \quad \dot{y}^\ell(t) = f^\ell(y^\ell(t), u(t)) \in \mathbb{R}^\ell \quad \text{for } t > 0, \quad y^\ell(0) = y_o^\ell \in \mathbb{R}^\ell,$$

where we have set  $y_o^\ell = \Psi^\top M y_o \in \mathbb{R}^\ell$  and

$$(3.4) \quad f^\ell(y^\ell, u) = \Psi^\top M f(\Psi y^\ell, u) \in \mathbb{R}^\ell \quad \text{for } (y^\ell, u) \in \mathbb{R}^\ell \times U_{\text{ad}};$$

i.e., no discrete interpolation method is used at the moment (compare, e.g., [10, 15]). From (3.4) and Assumption 2.1.1 we find that

$$\|f^\ell(y^\ell, u) - f^\ell(\tilde{y}^\ell, u)\|_2 \leq L_f^\ell \|y^\ell - \tilde{y}^\ell\|_2 \quad \text{for all } y^\ell, \tilde{y}^\ell \in \mathbb{R}^\ell \text{ and } u \in U_{\text{ad}}.$$

Here, the Lipschitz constant is given by  $L_f^\ell = L_f \|\Psi^\top M\|_2 \|\Psi\|_2$ , where, e.g.,  $\|\Psi\|_2$  stands for the largest singular value of the matrix  $\Psi$ . Furthermore,  $f^\ell(y^\ell, u)$  is bounded by the constant  $M_f \|\Psi^\top M\|_2$ , provided that the pair  $(\Psi y, u)$  belongs to  $\bar{\Omega} \times U_{\text{ad}}$ . Thus, there exists a unique solution  $y^\ell = y^\ell(u; y_o) \in \mathbb{Y}^\ell = W^{1,1}(0, \infty; \mathbb{R}^\ell)$  to (3.3) for any admissible control  $u \in U_{\text{ad}}$ . Let us introduce the linear orthogonal projection  $\mathcal{P}^\ell : \mathbb{R}^n \rightarrow V^\ell$  as

$$\mathcal{P}^\ell y = \Psi \Psi^\top M y = \sum_{i=1}^{\ell} \langle y, \psi_i \rangle_M \psi_i \quad \text{for } y \in \mathbb{R}^n.$$

We note that the error of a solution to (2.1) and (3.3) on a finite time horizon is of the order  $O(\sum_{i=\ell+1}^d \lambda_i)$ , which coincides with the approximation error (3.1).

**3.3. Reduced-order modelling for the optimal control problem.** Next we introduce the POD reduced-order model for  $(\hat{\mathbf{P}})$ . For given  $(u, y_o) \in U_{\text{ad}} \times \Omega$  let  $y^\ell = y^\ell(u; y_o) \in \mathbb{Y}^\ell$  denote the unique solution to (3.3). Then, the reduced POD cost is given by

$$\begin{aligned} \tilde{J}^\ell(u; y_o) &= J(y^\ell(u; y_o), u) = J(y^\ell, u) \\ &= \int_0^\infty g(\Psi y^\ell(t), u(t)) e^{-\lambda t} dt = \int_0^\infty g^\ell(y^\ell(t), u(t)) e^{-\lambda t} dt, \end{aligned}$$



where we have set

$$(3.5) \quad g^\ell(y^\ell, u) = g(\Psi y^\ell, u) \quad \text{for } (y^\ell, u) \in \mathbb{R}^\ell \times U_{\text{ad}}.$$

Then, the POD approximation for  $(\widehat{\mathbf{P}})$  reads as follows: for given  $y_\circ \in \Omega$  we consider

$$(\widehat{\mathbf{P}}^\ell) \quad \min \widehat{\mathcal{J}}^\ell(u; y_\circ) \quad \text{such that } u \in U_{\text{ad}}.$$

**4. A priori error for the HJB-POD approximation.** In this section we present the a priori error analysis for the coupling between the HJB equation and the POD method. Our first a priori error estimate is better from a theoretical point of view, whereas for the numerical realization the second a priori error estimate is much more appropriate. In the first estimate we assume to work in  $\mathbb{R}^\ell$  on a number of vertices which have been obtained by mapping the  $y_i$  nodes of  $\mathbb{R}^n$  into  $\mathbb{R}^\ell$ . The a priori error estimate, which we will present in section 4.1, depends on the POD approximation of the vertices  $\{y_i\}_{i=1}^{n_s}$ . However, even if the maximum distance between the  $y_i$  neighboring nodes is bounded by  $k$ , this clearly produces a nonuniform grid, where the distance between the neighboring nodes cannot be predicted a priori, since it depends on  $\Psi$ . The second error estimate takes into account a uniform grid of size  $K$  in  $\mathbb{R}^\ell$ . Here, we choose vertices  $\{y_i^\ell\}_{i=1}^{n_s} \subset \mathbb{R}^\ell$  in the POD subspace. However, the computation of the upper bound for the error is much more involved.

**4.1. First a priori error estimate.** We introduce two different POD approximations for the HJB equation. The first one is based on (2.9), where we project all vertices  $\{y_i\}_{i=1}^{n_s}$  into  $\mathbb{R}^\ell$  by setting

$$(4.1) \quad y_i^\ell = \Psi^\top M y_i \quad \text{for } i = 1, \dots, n_s.$$

Here we assume that  $y_i^\ell \neq y_j^\ell$  holds for  $i, j \in \{1, \dots, n_s\}$  with  $i \neq j$ . Moreover, we suppose that the points  $\{y_i^\ell\}_{i=1}^{n_s}$  are vertices of a regular triangulation of a polyhedron  $\overline{\Omega}^\ell \subset \mathbb{R}^\ell$ . Then, a POD discretization of (2.9) is given by

$$(4.2) \quad v_{hk}^\ell(y_i^\ell) = \min_{u \in U_{\text{ad}}} \{ (1 - \lambda h) v_{hk}^\ell(y_i^\ell + h f^\ell(y_i^\ell, u)) + h g^\ell(y_i^\ell, u) \}$$

for  $1 \leq i \leq n_s$ , and  $v_{hk}^\ell$  is a piecewise affine function on  $\overline{\Omega}^\ell$  having constant gradients in the interior of each simplex of the triangulation. We define the piecewise affine mapping  $\tilde{v}_{hk}^\ell : \overline{\Omega} \rightarrow \mathbb{R}$  by

$$\tilde{v}_{hk}^\ell(y) = v_{hk}^\ell(\Psi^\top M y) \quad \text{for all } y \in \overline{\Omega} \text{ with } \Psi^\top M y \in \overline{\Omega}^\ell.$$

Using the notation  $\mathcal{P}^\ell = \Psi \Psi^\top M \in \mathbb{R}^{n \times n}$ , (3.4), (3.5), and (4.1), we have

$$\begin{aligned} \tilde{v}_{hk}^\ell(y_i) &= v_{hk}^\ell(\Psi^\top M y_i) = v_{hk}^\ell(y_i^\ell) \\ &= \min_{u \in U_{\text{ad}}} \{ (1 - \lambda h) v_{hk}^\ell(y_i^\ell + h f^\ell(y_i^\ell, u)) + h g^\ell(y_i^\ell, u) \} \\ &= \min_{u \in U_{\text{ad}}} \{ (1 - \lambda h) v_{hk}^\ell(\Psi^\top M(y_i + h f(\mathcal{P}^\ell y_i, u))) + h g(\mathcal{P}^\ell y_i, u) \} \\ &= \min_{u \in U_{\text{ad}}} \{ (1 - \lambda h) \tilde{v}_{hk}^\ell(y_i + h f(\mathcal{P}^\ell y_i, u)) + h g(\mathcal{P}^\ell y_i, u) \} \end{aligned}$$

for  $1 \leq i \leq n_s$ . Thus, (4.2) can be equivalently expressed as

$$(4.3) \quad \tilde{v}_{hk}^\ell(y_i) = \min_{u \in U_{\text{ad}}} \{ (1 - \lambda h) \tilde{v}_{hk}^\ell(y_i + h f(\mathcal{P}^\ell y_i, u)) + h g(\mathcal{P}^\ell y_i, u) \}$$

for  $1 \leq i \leq n_s$ . The following result measures the error between a solution to (2.5) and a solution to (4.3). The proof is similar to the proof of Theorem 1.3 in [18] and requires an invariance condition which will be discussed later in Remark 4.2.

PROPOSITION 4.1. *Assume that Assumption 2.1, (2.7), and  $\lambda > L_f$  hold. Let  $v_h$  and  $\tilde{v}_{hk}^\ell$  be the solutions of (2.5) and (4.3), respectively, and let the invariance condition*

$$(4.4) \quad y_i + hf(\mathcal{P}^\ell y_i, u) \in \bar{\Omega} \quad \text{for } i = 1, \dots, n_s \text{ and for all } u \in U_{\text{ad}}$$

be satisfied. Then, there exist two constants  $\widehat{C}_0, \widehat{C}_1$  such that

$$(4.5) \quad \|v_h - \tilde{v}_{hk}^\ell\|_{C(\bar{\Omega})} \leq \widehat{C}_0 \frac{k}{h} + \widehat{C}_1 \left( \sum_{i=1}^{n_s} \|y_i - \mathcal{P}^\ell y_i\|_2^2 \right)^{1/2} \quad \text{for any } h \in \left[ 0, \frac{1}{\lambda} \right).$$

*Proof.* For any  $y \in \Omega$  there are real coefficients  $\mu_i = \mu_i(y)$ ,  $1 \leq i \leq n_s$ , of the convex combination representation of  $y$  satisfying

$$y = \sum_{i=1}^{n_s} \mu_i y_i, \quad 0 \leq \mu_i \leq 1, \quad \text{and} \quad \sum_{i=1}^{n_s} \mu_i = 1.$$

Since  $\tilde{v}_{hk}^\ell$  is piecewise affine, we obtain  $\tilde{v}_{hk}^\ell(y) = \sum_{i=1}^{n_s} \mu_i \tilde{v}_{hk}^\ell(y_i)$ . Thus, we have

$$(4.6) \quad |v_h(y) - \tilde{v}_{hk}^\ell(y)| \leq \left| \sum_{i=1}^{n_s} \mu_i (v_h(y) - v_h(y_i)) \right| + \left| \sum_{i=1}^{n_s} \mu_i (v_h(y_i) - \tilde{v}_{hk}^\ell(y_i)) \right|.$$

From  $y \in \bar{\Omega}$  we infer that there exists an index  $j$  with  $y \in \bar{\mathcal{S}}_j \subset \bar{\Omega}$ . Let  $J_j = \{i_1, \dots, i_k\} \subset \{1, \dots, n_s\}$  denote the index subset such that  $y_i \in \bar{\mathcal{S}}_j$  holds for  $i \in J_j$ . Then  $\mu_i = 0$  holds for all  $i \notin J_j$ . Moreover,  $\sum_{i=1}^{n_s} \mu_i = \sum_{i \in J_j} \mu_i = 1$  and  $\|y - y_i\|_2 \leq k$  for any  $i \in J_j$ . From (2.6) we have

$$(4.7) \quad \sum_{i=1}^{n_s} \mu_i |v_h(y) - v_h(y_i)| = \sum_{i \in J_j} \mu_i |v_h(y) - v_h(y_i)| \leq \frac{L_g}{\lambda - L_f} k$$

for  $h \in [0, 1/\lambda)$ . Using (4.3) and (2.5), we have

$$(4.8) \quad \begin{aligned} & v_h(y_i) - \tilde{v}_{hk}^\ell(y_i) \\ & \leq v_h(y_i) - (1 - \lambda h) \tilde{v}_{hk}^\ell(y_i + hf(\mathcal{P}^\ell y_i, \bar{u}_{hk}^{\ell,i})) + hg(\mathcal{P}^\ell y_i, \bar{u}_{hk}^{\ell,i}) \\ & \leq (1 - \lambda h) \left( v_h(y_i + hf(y_i, \bar{u}_{hk}^{\ell,i})) - \tilde{v}_{hk}^\ell(y_i + hf(\mathcal{P}^\ell y_i, \bar{u}_{hk}^{\ell,i})) \right) \\ & \quad + h(g(y_i, \bar{u}_{hk}^{\ell,i}) - g(\mathcal{P}^\ell y_i, \bar{u}_{hk}^{\ell,i})), \end{aligned}$$

where  $\bar{u}_{hk}^{\ell,i} \in U_{\text{ad}}$  is defined as

$$(4.9) \quad \bar{u}_{hk}^{\ell,i} = \operatorname{argmin}_{u \in U_{\text{ad}}} \{ (1 - \lambda h) \tilde{v}_{hk}^\ell(y_i + hf(\mathcal{P}^\ell y_i, u)) + hg(\mathcal{P}^\ell y_i, u) \}.$$

Applying (2.6) again, we deduce that

$$|v_h(y_i + hf(y_i, \bar{u}_{hk}^{\ell,i})) - v_h(y_i + hf(\mathcal{P}^\ell y_i, \bar{u}_{hk}^{\ell,i}))| \leq \frac{hL_gL_f}{\lambda - L_f} \|y_i - \mathcal{P}^\ell y_i\|_2$$

for  $1 \leq i \leq n_S$  and  $h \in [0, 1/\lambda)$ . Hence, from (4.4) it follows that

$$\begin{aligned} & v_h(y_i + hf(y_i, \bar{u}_{hk}^{\ell,i})) - \tilde{v}_{hk}^\ell(y_i + hf(\mathcal{P}^\ell y_i, \bar{u}_{hk}^{\ell,i})) \\ & \leq \left( v_h(y_i + hf(y_i, \bar{u}_{hk}^{\ell,i})) - v_h(y_i + hf(\mathcal{P}^\ell y_i, \bar{u}_{hk}^{\ell,i})) \right) \\ & \quad + \left( v_h(y_i + hf(\mathcal{P}^\ell y_i, \bar{u}_{hk}^{\ell,i})) - \tilde{v}_{hk}^\ell(y_i + hf(\mathcal{P}^\ell y_i, \bar{u}_{hk}^{\ell,i})) \right) \\ & \leq \frac{hL_g L_f}{\lambda - L_f} \|y_i - \mathcal{P}^\ell y_i\|_2 + \|v_h - \tilde{v}_{hk}^\ell\|_{C(\bar{\Omega})} \end{aligned}$$

for  $1 \leq i \leq n_S$  and  $h \in [0, 1/\lambda)$ . Using the inequality

$$h(g(y_i, \bar{u}_{hk}^{\ell,i}) - g(\mathcal{P}^\ell y_i, \bar{u}_{hk}^{\ell,i})) \leq hL_g \|y_i - \mathcal{P}^\ell y_i\|_2,$$

we derive from (4.8) that

$$v_h(y_i) - \tilde{v}_{hk}^\ell(y_i) \leq \tilde{C}_1 h \|y_i - \mathcal{P}^\ell y_i\|_2 + (1 - \lambda h) \|v_h - \tilde{v}_{hk}^\ell\|_{C(\bar{\Omega})}$$

for  $1 \leq i \leq n_S$  and  $h \in [0, 1/\lambda)$  with  $\tilde{C}_1 = L_g(L_f/(\lambda - L_f) + 1)$ . By interchanging the role of  $v_h$  and  $\tilde{v}_{hk}^\ell$  in (4.8), we derive

$$(4.10) \quad |v_h(y_i) - \tilde{v}_{hk}^\ell(y_i)| \leq \tilde{C}_1 h \|y_i - \mathcal{P}^\ell y_i\|_2 + (1 - \lambda h) \|v_h - \tilde{v}_{hk}^\ell\|_{C(\bar{\Omega})}$$

for  $1 \leq i \leq n_S$  and  $h \in [0, 1/\lambda)$ . Note that  $0 \leq \sum_{i=1}^{n_S} \mu_i^2 \leq \sum_{i=1}^{n_S} \mu_i = 1$  holds for the coefficients in the convex combination representation. Inserting (4.7) and (4.10) into (4.6), we find

$$\begin{aligned} & |v_h(y) - \tilde{v}_{hk}^\ell(y)| \\ & \leq (1 - \lambda h) \|v_h - \tilde{v}_{hk}^\ell\|_{C(\bar{\Omega})} + \tilde{C}_0 k + \tilde{C}_1 h \sum_{i=1}^{n_S} \mu_i \|y_i - \mathcal{P}^\ell y_i\|_2 \\ (4.11) \quad & \leq (1 - \lambda h) \|v_h - \tilde{v}_{hk}^\ell\|_{C(\bar{\Omega})} + \tilde{C}_0 k + \tilde{C}_1 h \left( \sum_{i=1}^{n_S} \|y_i - \mathcal{P}^\ell y_i\|_2^2 \right)^{1/2} \end{aligned}$$

for  $h \in [0, 1/\lambda)$  with  $\tilde{C}_0 = L_g/(\lambda - L_f)$ , which implies (4.5) with the constants  $\hat{C}_i = \tilde{C}_i/\lambda$ ,  $i = 0, 1$ .  $\square$

*Remark 4.2.* Let us give sufficient conditions for (4.4). First, we observe that for any  $i \in \{1, \dots, n_S\}$  and  $u \in U_{ad}$  we have

$$y_i + hf(\mathcal{P}^\ell y_i, u) = y_i + hf(y_i, u) + h(f(\mathcal{P}^\ell y_i, u) - f(y_i, u)).$$

To ensure (4.4) we replace (2.7) by the stronger assumption

$$y + hf(y, u) \in \text{int } \Omega \quad \text{for all } y \in \bar{\Omega} \text{ and } u \in U_{ad},$$

where  $\text{int } \Omega$  stands for the (open) interior of the set  $\Omega$ , and we have  $y_i + hf(y_i, u) \in \text{int } \Omega$  for any  $i \in \{1, \dots, n_S\}$ . Moreover, Assumption 2.1.1 implies that

$$\|f(\mathcal{P}^\ell y_i, u) - f(y_i, u)\|_2 \leq L_f \|\mathcal{P}^\ell y_i - y_i\|_2 \quad \text{for all } u \in U_{ad}$$

holds. Consequently, if either the mesh size  $h$  or  $\|\mathcal{P}^\ell y_i - y_i\|_2$  is sufficiently small, the norm of the vector  $h(f(\mathcal{P}^\ell y_i, u) - f(y_i, u))$  can be made sufficiently small so that  $y_i + hf(\mathcal{P}^\ell y_i, u) \in \bar{\Omega}$ .

From Theorem 2.3 and Proposition 4.1 we derive the following a priori error estimate.

**THEOREM 4.3.** *Assume that Assumption 2.1, (2.7), and (4.4) hold. Let  $v$  and  $\tilde{v}_{hk}^\ell$  be the solutions of (2.4) and (4.3), respectively. If  $\lambda > \max\{L_f, L_g\}$ , then there exist constants  $c_0, c_1, c_2 \geq 0$  such that*

$$(4.12) \quad \|v - \tilde{v}_{hk}^\ell\|_{C(\bar{\Omega})} \leq Ch + \hat{C}_0 \frac{k}{h} + \hat{C}_1 \left( \sum_{i=1}^{n_s} \|y_i - \mathcal{P}^\ell y_i\|_2^2 \right)^{1/2}$$

for any  $h \in [0, 1/\lambda)$ , where the positive constants  $C, \hat{C}_0,$  and  $\hat{C}_1$  are given by Theorem 2.3 and Proposition 4.1.

*Remark 4.4.* The a priori error estimate presented in Theorem 4.3 is natural, because it combines the discretization error between  $v$  and  $v_{hk}$  (compare (2.11)) with the POD approximation quality for the (finitely many) vertices  $\{y_i\}_{i=1}^{n_s}$ . In particular, if we determine the POD basis by solving

$$\begin{cases} \min \sum_{i=1}^{n_s} \left\| y_i - \sum_{j=1}^{\ell} \langle y_i, \psi_j \rangle_2 \psi_j \right\|_2^2 \\ \text{such that } \{\psi_i\}_{i=1}^{\ell} \subset \mathbb{R}^n \text{ and } \langle \psi_i, \psi_j \rangle_2 = \delta_{ij}, \quad 1 \leq i, j \leq \ell, \end{cases}$$

we get the a priori error estimate

$$\|v - \tilde{v}_{hk}^\ell\|_{C(\bar{\Omega})} \leq Ch + \hat{C}_0 \frac{k}{h} + \hat{C}_1 \left( \sum_{i=\ell+1}^{n_s} \lambda_i \right)^{1/2}.$$

However, the POD grid points  $\{y_i^\ell\}_{i=1}^{n_s}$  are not well distributed in general, which is disadvantageous for the numerical realization.

**4.2. Second a priori error estimate.** From a numerical point of view (4.2) is not appropriate, because in general the grid points  $\{y_i^\ell\}_{i=1}^{n_s}$  are not uniformly distributed in  $\mathbb{R}^\ell$  and their distribution will strongly depend on  $\Psi$ . Therefore, we define a second POD discretization of the HJB equations where we have an explicit bound on the distance between the neighboring nodes. Clearly in this case we will need an interpolation operator defined on the grid. (Typically, this will be a piecewise linear interpolation operator.) With (2.7) holding, we assume that there exists a bounded polyhedron  $\Omega^\ell \subset \mathbb{R}^\ell$  satisfying

$$(4.13) \quad \Psi^\top My \in \text{int } \Omega^\ell \quad \text{for all } y \in \bar{\Omega}.$$

*Remark 4.5.* Condition (4.13) implies that

$$y^\ell + hf^\ell(y^\ell, u) \in \bar{\Omega}^\ell,$$

provided the step size  $h$  or  $\|\Psi\Psi^\top My - y\|_2$  is sufficiently small. In fact, let  $y \in \bar{\Omega}$ , let  $u \in U_{ad}$  be arbitrarily chosen, and set  $y^\ell = \Psi^\top My \in \mathbb{R}^\ell$ . Then,

$$\begin{aligned} y^\ell + hf^\ell(y^\ell, u) &= \Psi^\top My + h\Psi^\top Mf(\Psi\Psi^\top My, u) \\ &= \Psi^\top M(y + hf(y, u)) + h\Psi^\top M(f(\Psi\Psi^\top My, u) - f(y, u)). \end{aligned}$$

We infer from (2.7) that  $z = y + hf(y, u) \in \bar{\Omega}$  holds. Hence, by (4.13), we have  $\Psi^T Mz \in \text{int } \Omega^\ell$ . Furthermore, we derive from

$$\|h\Psi^T M(f(\Psi\Psi^T My, u) - f(y, u))\|_2 \leq hL_f \|\Psi^T M\|_2 \|\Psi\Psi^T My - y\|_2$$

and  $\text{span}\{\psi_1, \dots, \psi_n\} = \mathbb{R}^n$  that  $y^\ell + hf^\ell(y^\ell, u) \in \bar{\Omega}^\ell$  holds for step size  $h$  or  $\|\Psi\Psi^T My - y\|_2$  sufficiently small. If  $M = \text{Id} \in \mathbb{R}^{n \times n}$  holds, we have  $\|\Psi^T M\|_2 = 1$ .

Let  $\{\mathcal{S}_j^\ell\}_{j=1}^{m_s}$  be a family of simplices which defines a regular triangulation of the polyhedron  $\Omega^\ell$  (see, e.g., [24]) such that

$$(4.14) \quad \bar{\Omega}^\ell = \bigcup_{j=1}^{m_s} \mathcal{S}_j^\ell \quad \text{and} \quad K = \max_{1 \leq j \leq m_s} (\text{diam } \mathcal{S}_j^\ell).$$

Let  $V^K$  be the space of piecewise affine functions from  $\bar{\Omega}^\ell$  to  $\mathbb{R}$  which are continuous in  $\bar{\Omega}^\ell$  having constant gradients in the interior of any simplex  $\mathcal{S}_j^\ell$  of the triangulation. Then, we introduce the following POD scheme for the HJB equations:

$$(4.15) \quad v_{hK}^\ell(y_i^\ell) = \min_{u \in U_{\text{ad}}} \{(1 - \lambda h)v_{hK}^\ell(y_i^\ell + hf^\ell(y_i^\ell, u)) + hg^\ell(y_i^\ell, u)\}$$

for any vertex  $y_i^\ell \in \bar{\Omega}^\ell$ . Throughout this paper we assume that we have  $n_s$  vertices  $y_1^\ell, \dots, y_{n_s}^\ell$ . We set

$$(4.16) \quad y_i = \Psi y_i^\ell \in \mathbb{R}^n \quad \text{for } 1 \leq i \leq n_s$$

and define

$$\tilde{v}_{hK}^\ell(y) = v_{hK}^\ell(\Psi^T My) \quad \text{for all } y \in \bar{\Omega}.$$

Recall that (4.13) ensures that  $\Psi^T My \in \text{int } \Omega^\ell$  for any  $y \in \bar{\Omega}$ . Moreover,  $y_i = \Psi y_i^\ell$  and  $\Psi^T M\Psi = \text{Id} \in \mathbb{R}^{\ell \times \ell}$  implies that

$$\tilde{v}_{hK}^\ell(y_i) = v_{hK}^\ell(\Psi^T My_i) = v_{hK}^\ell(y_i^\ell) \quad \text{for } 1 \leq i \leq n_s.$$

Using  $\Psi^T M\Psi y_i^\ell = y_i^\ell$ , (4.15), (3.4), (3.5), and (4.16), we obtain

$$\begin{aligned} \tilde{v}_{hK}^\ell(y_i) &= v_{hK}^\ell(y_i^\ell) = \min_{u \in U_{\text{ad}}} \{(1 - \lambda h)v_{hK}^\ell(y_i^\ell + hf^\ell(y_i^\ell, u)) + hg^\ell(y_i^\ell, u)\} \\ &= \min_{u \in U_{\text{ad}}} \{(1 - \lambda h)v_{hK}^\ell(\Psi^T M(\Psi y_i^\ell + hf(\Psi y_i^\ell, u))) + hg(\Psi y_i^\ell, u)\} \\ &= \min_{u \in U_{\text{ad}}} \{(1 - \lambda h)v_{hK}^\ell(\Psi^T M(y_i + hf(y_i, u))) + hg(y_i, u)\} \\ &= \min_{u \in U_{\text{ad}}} \{(1 - \lambda h)\tilde{v}_{hK}^\ell(y_i + hf(y_i, u)) + hg(y_i, u)\} \quad \text{for } 1 \leq i \leq n_s. \end{aligned}$$

Thus, (4.15) can be written as

$$(4.17) \quad \tilde{v}_{hK}^\ell(y_i) = \min_{u \in U_{\text{ad}}} \{(1 - \lambda h)\tilde{v}_{hK}^\ell(y_i + hf(y_i, u)) + hg(y_i, u)\}$$

for  $1 \leq i \leq n_s$ .

**PROPOSITION 4.6.** *Assume that Assumption 2.1, (2.7), and (4.13) hold. Let  $v_h$  and  $\tilde{v}_{hK}^\ell$  be the solutions of (2.5) and (4.17). Let*

$$(4.18) \quad \Psi^T M(y + hf(\mathcal{P}^\ell y, u)) \in \bar{\Omega}^\ell \quad \text{for all } y \in \bar{\Omega} \text{ and } u \in U_{\text{ad}}.$$

be satisfied. Let the step size  $K$  be defined as in (4.14). For  $\lambda > L_f$  there exists a constant  $c_0$  such that

$$(4.19) \quad \|v_h - \tilde{v}_{hk}^\ell\|_{C(\bar{\Omega})} \leq c_0 \left( \|\Psi\|_2 \frac{K}{h} + \sup_{y \in \bar{\Omega}} \|y - \mathcal{P}^\ell y\|_2 \frac{1}{h} \right)$$

for any  $h \in [0, 1/\lambda)$ .

*Proof.* Let  $y \in \bar{\Omega}$  be chosen arbitrarily. We set  $y^\ell = \Psi^\top M y$ . By (4.13) we have  $y^\ell \in \text{int } \Omega^\ell$ . In contrast to the proof of Theorem 4.3, here we consider a convex combination representation for the point  $y^\ell$  in  $\mathbb{R}^\ell$ . There are real coefficients  $\mu_i^\ell = \mu_i^\ell(y^\ell)$ ,  $1 \leq i \leq n_s$ , satisfying

$$y^\ell = \sum_{i=1}^{n_s} \mu_i^\ell y_i^\ell, \quad 0 \leq \mu_i^\ell \leq 1, \quad \text{and} \quad \sum_{i=1}^{n_s} \mu_i^\ell = 1.$$

Since  $v_{hK}^\ell$  is piecewise affine we have  $v_{hK}(y^\ell) = \sum_{i=1}^{n_s} \mu_i^\ell v_{hK}^\ell(y_i^\ell)$ . Using  $y_i = \Psi y_i^\ell$ , we have

$$(4.20) \quad \begin{aligned} |v_h(y) - \tilde{v}_{hk}^\ell(y)| &\leq |v_h(y) - v_h(\mathcal{P}^\ell y)| + \left| \sum_{i=1}^{n_s} \mu_i^\ell (v_h(\mathcal{P}^\ell y) - v_h(y_i)) \right| \\ &\quad + \left| \sum_{i=1}^{n_s} \mu_i^\ell (v_h(y_i) - v_{hK}^\ell(y_i^\ell)) \right|. \end{aligned}$$

By (2.6) the first term on the right-hand side of (4.20) can be bounded as follows:

$$(4.21) \quad |v_h(y) - v_h(\mathcal{P}^\ell y)| \leq \frac{L_g}{\lambda - L_f} \|y - \mathcal{P}^\ell y\|_2 \quad \text{for all } h \in \left[0, \frac{1}{\lambda}\right).$$

Furthermore, there exists an index  $j$  with  $y \in \bar{\mathcal{S}}_j \subset \bar{\Omega}^\ell$ . Let  $\mathcal{J}_j = \{i_1, \dots, i_k\} \subset \{1, \dots, n_s\}$  denote the index subset such that  $y^\ell \in \bar{\mathcal{S}}_j$  holds for  $i \in \mathcal{J}_j$ . Then,  $\mu_i^\ell = 0$  holds for all  $i \notin \mathcal{J}_j$ . Moreover,  $\sum_{i=1}^{n_s} \mu_i^\ell = \sum_{i \in \mathcal{J}_j} \mu_i^\ell = 1$  and  $\|y^\ell - y_i^\ell\|_2 \leq K$  for any  $i \in \mathcal{J}_j$ . Recall that  $\mathcal{P}^\ell y = \Psi \Psi^\top M y = \Psi y^\ell$  holds. Again using (2.6), we find

$$(4.22) \quad \sum_{i=1}^{n_s} \mu_i^\ell |v_h(\mathcal{P}^\ell y) - v_h(y_i)| = \sum_{i \in \mathcal{J}_j} \mu_i^\ell |v_h(\Psi y^\ell) - v_h(\Psi y_i^\ell)| \leq \frac{L_g \|\Psi\|_2}{\lambda - L_f} K$$

for  $h \in [0, 1/\lambda)$ . Using (4.17) and (2.5), we have

$$\begin{aligned} v_h(y_i) - v_{hK}^\ell(y_i^\ell) &= v_h(y_i) - \tilde{v}_{hK}^\ell(y_i) \\ &\leq v_h(y_i) - (1 - \lambda h) \tilde{v}_{hK}^\ell(y_i + hf(y_i, \bar{u}_{hK}^{\ell,i})) - hg(y_i, \bar{u}_{hK}^{\ell,i}) \\ &\leq (1 - \lambda h) \left( v_h(y_i + hf(y_i, \bar{u}_{hK}^{\ell,i})) - \tilde{v}_{hK}^\ell(y_i + hf(y_i, \bar{u}_{hK}^{\ell,i})) \right) \\ &\leq (1 - \lambda h) \|v_h - \tilde{v}_{hK}^\ell\|_{C(\bar{\Omega})}, \end{aligned}$$

where  $\bar{u}_{hK}^{\ell,i} \in U_{\text{ad}}$  is defined as

$$\bar{u}_{hK}^{\ell,i} = \underset{u \in U_{\text{ad}}}{\text{argmin}} \left\{ (1 - \lambda h) \tilde{v}_{hK}^\ell(y_i + hf(y_i, u)) + hg(y_i, u) \right\},$$

which is similar to (4.9), but not equal to it. By interchanging the role of  $v_h$  and  $v_{hK}^\ell$ , we find

$$(4.23) \quad |v_h(y_i) - v_{hk}^\ell(y_i^\ell)| \leq (1 - \lambda h) \|v_h - \tilde{v}_{hK}^\ell\|_{C(\bar{\Omega})}.$$

Inserting (4.21), (4.22), and (4.23) into (4.20), we derive (4.19) with  $c_0 = \frac{L_g}{\lambda(\lambda - L_f)}$ .  $\square$

*Remark 4.7.*

1. In Remark 4.5 we give a sufficient condition for (4.18). If (4.13) holds and the step size  $h$  or  $\|y - \mathcal{P}^\ell y\|_2$  is sufficiently small, then (4.18) is satisfied. Recall that  $\|y - \mathcal{P}^\ell y\|_2 \rightarrow 0$  for any  $y \in \bar{\Omega}$ , provided  $\ell \rightarrow n$ .
2. We should balance

$$K \sim \sup_{y \in \bar{\Omega}} \|y - \mathcal{P}^\ell y\|_2$$

in order to get a rate  $K/h$  for the convergence.

3. Let us comment on the term  $\sup_{y \in \bar{\Omega}} \|y - \mathcal{P}^\ell y\|_2$  in (4.19). For the numerical realization we do not have  $\Omega$  at hand. Therefore, we suggest the following approach: In the context of section 3.1 we compute the discrete solutions  $y_j^\nu \in \mathbb{R}^n$ ,  $j = 1, \dots, n_T$ , to (2.1) for different controls  $u^\nu$  and initial conditions  $y_0^\nu$  for  $\nu = 1, \dots, p$ . Then we suppose that all elements in the bounded set  $\bar{\Omega}$  can be expressed by an element in the snapshot subspace  $\mathcal{V}^{n_T} \subset \mathbb{R}^n$ . If the POD basis is determined by  $(\mathbf{P}_{n_T}^\ell)$ , then we can estimate the term  $\sup_{y \in \mathcal{V}^{n_T}} \|y - \mathcal{P}^\ell y\|_2$  in terms of the decay of the POD eigenvalues; compare (3.2).

Combining Theorem 2.3 and Proposition 4.6. we obtain the following result.

**THEOREM 4.8.** *Assume that Assumption 2.1, (2.7), (4.13), and (4.18) hold. Let  $v$  and  $\tilde{v}_{hK}^\ell$  be the solutions of (2.4) and (4.17), respectively. If  $\lambda > \max\{L_f, L_g\}$ , then*

$$(4.24) \quad \|v - \tilde{v}_{hK}^\ell\|_{C(\bar{\Omega})} \leq Ch + c_0 \left( \|\Psi\|_2 \frac{K}{h} + \sup_{y \in \bar{\Omega}} \|y - \mathcal{P}^\ell y\|_2 \frac{1}{h} \right)$$

for any  $h \in [0, 1/\lambda)$ , where the positive constant  $C$  and  $c_0$  have been introduced in Theorems 2.3 and 4.6, respectively.

*Remark 4.9.* Let us comment on the differences between the a priori error estimates (4.12) and (4.24):

1. Both estimates involve terms depending on  $h$  and on  $k/h$  or  $K/h$ . Note that  $\|\Psi\|_2 = 1$  if we choose  $M = \text{Id}$  in the computation of the POD basis.
2. Using  $\sum_{i=1}^{n_s} \mu_i = 1$ , we can replace (4.11) by

$$|v_h(y) - \tilde{v}_{hk}^\ell(y)| \leq (1 - \lambda h) \|v_h - \tilde{v}_{hk}^\ell\|_{C(\bar{\Omega})} + \tilde{C}_0 k + \tilde{C}_1 h \max_{1 \leq i \leq n_s} \|y_i - \mathcal{P}^\ell y_i\|_2$$

for  $h \in [0, 1/\lambda)$  with  $\tilde{C}_0 = L_g/(\lambda - L_f)$  and  $\tilde{C}_1 = L_g(L_f/(\lambda - L_f) + 1)$ . Then, (4.12) becomes

$$(4.25) \quad \|v - \tilde{v}_{hk}^\ell\|_{C(\bar{\Omega})} \leq Ch + \hat{C}_0 \frac{k}{h} + \hat{C}_1 \max_{1 \leq i \leq n_s} \|y_i - \mathcal{P}^\ell y_i\|_2$$

for any  $h \in [0, 1/\lambda)$  with the same constants  $C$ ,  $\hat{C}_0$ , and  $\hat{C}_1$ . Now we compare the POD approximation errors in (4.24) and (4.25). In (4.25) the last term

is not divided by  $h$ . Furthermore, in (4.24) the term  $\|y - \mathcal{P}^\ell y\|_2$  has to be small for all  $y \in \bar{\Omega}$ , whereas in (4.25) this is needed only for the vertices  $y_1, \dots, y_{n_s} \in \bar{\Omega}$ . In order to get convergence for  $h \rightarrow 0$  from (4.24) one has to guarantee that  $K = o(h)$  and  $\sup_{y \in \bar{\Omega}} \|y - \mathcal{P}^\ell y\|_2 = o(h)$ . In contrast, a convergence for  $h \rightarrow 0$  holds for (4.25), provided  $k = o(h)$  and

$$\lim_{h \rightarrow 0} \max_{1 \leq i \leq n_s} \|y_i - \mathcal{P}^\ell y_i\|_2 = 0.$$

Recall that the choice of the vertices  $y_i, i = 1, \dots, n_s$ , depends on  $h$ ; cf. (2.8). Anyway, as we will see in our numerical examples, the method seems to be rather efficient also for larger  $K$ .

**5. Practical implementation of the algorithm.** In this section we present an algorithm for the HJB equation based on the POD a priori analysis presented in section 4.2. The estimate in Theorem 4.8 suggests the following steps:

(1) *Time discretization.* First the infinite time horizon  $[0, \infty)$  has to be replaced by a finite one. Thus, we choose  $t_e \gg 0$  sufficiently large so that it has little effect on the numerical results and define a (possibly nonequidistant) grid in  $[0, t_e]$  by  $0 = t_1 < t_2 < \dots < t_{n_T} = t_e$ .

(2) *Snapshots computation.* Let us suppose that the set of admissible controls  $U_{ad}$  is one-dimensional, i.e.,  $m = 1$ , and that  $U_{ad}$  given by choosing a discrete set  $U_{ad} = \{u_1, \dots, u_p\} \subset U = \mathbb{R}$ . To solve (2.1) we apply the implicit Euler method on the time grid  $\{t_j\}_{j=1}^{n_T}$ . By  $y_j^\nu \approx y^\nu(t_j) \in \mathbb{R}^n, 1 \leq j \leq n_T$  and  $1 \leq \nu \leq p$ , we denote the computed implicit Euler approximation of the solution to (2.1) at time instance  $t_j$  for the controls  $u^\nu(t) = u_\nu$  for all  $t \in [0, t_e]$  and  $1 \leq \nu \leq p$ . This idea can be generalized to a higher-dimensional control set.

(3) *Rank  $\ell$  of the POD basis.* In  $(\mathbf{P}_{n_T}^\ell)$  we choose  $M$  as the identity matrix since we deal with finite difference approximation and  $\alpha_j^{n_T} = 1$  for  $j = 1, \dots, n_T$ . We note that a finite element approximation leads to a mass matrix  $M$  different from the identity.

The rank  $\ell$  of the POD basis  $\{\psi_i^{n_T}\}_{i=1}^\ell$  is chosen such that we can show the decay of the error when we increase  $\ell$ . In this paper we choose  $\ell \in \{2, 3, 4\}$ . A heuristic way to select the number of POD basis functions  $\ell$  is given by the error estimate (4.24). In particular, as explained in Remark 4.9, the term  $\sup_{y \in \bar{\Omega}} \|y - \mathcal{P}^\ell y\|_2$  should be below a given tolerance, chosen accurately. This can be achieved with a clever selection of the value of  $\ell$  since the term goes to 0 when  $\ell \rightarrow \infty$ ; compare the right panel of Figure 6.6 below.

(4) *Computation of the polyhedron  $\Omega^\ell$ .* We first define all the POD grid points as the projection of the snapshots, previously computed,  $y_j^\ell = \Psi^\top y_j^\nu \in \mathbb{R}^\ell$  for  $1 \leq j \leq m_y$ . Then, a simple choice is to consider the hypercube  $\Omega^\ell = [a_1, b_1] \times \dots \times [a_\ell, b_\ell] \subset \mathbb{R}^\ell$ , where we set

$$a_i = \min \{(y_1^\ell)_i, \dots, (y_{m_y}^\ell)_i\}, \quad b_i = \max \{(y_1^\ell)_i, \dots, (y_{m_y}^\ell)_i\},$$

for  $1 \leq i \leq \ell$ . It follows that  $y_j^\ell \in \Omega^\ell$  for  $1 \leq j \leq m_y$ . Then, when the domain  $\Omega^\ell$  is obtained, we build an equidistant grid with step size computed as explained in Remark 4.7. We note that  $\Omega^\ell$  should be large enough to contain all possible trajectories and satisfy the invariance condition (6.5) for the reduced coordinates. This is also the reason we compute several snapshots in order to have a sufficiently accurate overview of the problem.



(5) *Computation of the value function  $v_{hK}^\ell$ .* The piecewise linear value function  $v_{hK}^\ell$  is determined on the vertices  $y_i$  for  $1 \leq i \leq n_s$  of the domain  $\Omega^\ell$ . Since the reduced-order approach yields a small  $\ell < 10$ , we are able to perform a standard fixed point iteration method, e.g., the value iteration method. We also refer the reader to faster algorithms such as those in [2] and the references therein.

(6) *Feedback law and closed-loop control.* We compute the value function  $\tilde{v}_{hK}^\ell(y) = v_{hK}(\Psi^\top y)$  satisfying (4.2) at each grid point  $y = y_i$  for  $1 \leq i \leq m_y$ . At any grid point  $y_i$  we store the associated optimal control  $\bar{u}_{hK}^{\ell,i} \in U_{ad}$  solving

$$u_{hK}^{\ell,i} := \operatorname{argmin}_{u \in U_{ad}} \{ (1 - \lambda h) \tilde{v}_{hK}^\ell(y_i + hf(\mathcal{P}^\ell y_i, u)) + hg(\mathcal{P}^\ell y_i, u) \}.$$

Then, the (suboptimal) feedback operator  $\Phi^\ell : \bar{\Omega} \rightarrow U_{ad}$  is defined as

$$\Phi^\ell(y) = \sum_{i=1}^{m_y} \mu_i \bar{u}_{hK}^{\ell,i} \quad \text{for } y \in \bar{\Omega},$$

where the coefficients  $\{\mu_i\}_{i=1}^{m_y}$  are given by the convex combination

$$y = \sum_{i=1}^{m_y} \mu_i y_i, \quad 0 \leq \mu_i \leq 1, \quad \sum_{i=1}^{m_y} \mu_i = 1.$$

Now the closed-loop system for (2.1) is

$$(5.1) \quad \dot{y}(t) = f(y(t), \Phi^\ell(y(t))) \in \mathbb{R}^n \quad \text{for } t > 0, \quad y(0) = y_o \in \mathbb{R}^n.$$

Equation (5.1) is solved by a semi-implicit Euler scheme, where the second argument  $\Phi^\ell(y(t))$  is evaluated at the previous time step. We note that at every time step  $t_i$  we plug the suboptimal control  $u_{h,K}^{\ell,i}$  into (5.1) and then project into the POD space in order to have the next initial condition. The algorithm is summarized below.

---

**Algorithm 5.1** HJB-POD feedback control.

---

**Require:** distance  $K$ , step size  $h$ , final time  $t_e$ , time grid  $\{t_j\}_{j=1}^{n_T}$ , discrete control

- set  $U_{ad} = \{u_1, \dots, u_p\} \subset \mathbb{R}$ ;
  - 1: Set  $Y = []$  and  $\Delta = K$ ;
  - 2: **for**  $\nu = 1, \dots, p$  **do**
  - 3:   Compute approximation  $\{y_j^\nu\}_{j=1}^{n_T}$  for the solution to (2.1) with  $u \equiv u_\nu$ ;
  - 4:   Set  $Y = [Y \mid y_1^\nu, \dots, y_{n_T}^\nu] \in \mathbb{R}^{n \times (\nu n_T)}$ ;
  - 5: **end for**
  - 6: Set  $m_y = pn_T$  and  $Y = [y_1, \dots, y_{m_y}] \in \mathbb{R}^{n \times m_y}$ ;
  - 7: Determine a POD basis of rank  $\ell$  by solving  $(\mathbf{P}_{n_T}^\ell)$ ;
  - 8: Choose  $\Omega^\ell$  and compute the reduced value function  $\tilde{v}_{hK}^\ell$ ;
  - 9: Compute the suboptimal control and the optimal trajectory;
- 

**6. Numerical tests.** In this section we present our numerical tests. First let us describe the optimal control problem in detail. For numerical reasons, we have to consider a finite time horizon, so that we choose a sufficiently large  $t_e > 0$ . In our numerical experiments we choose  $t_e$  large enough such that it does not change our numerical results. The governing nonlinear PDE with a finite time horizon is given

by

$$(6.1) \quad \begin{aligned} z_t - \varepsilon z_{xx} + \gamma z_x + \mu(z - z^3) &= bu & \text{in } \omega \times (0, t_e), \\ z(\cdot, 0) &= z_o & \text{in } \omega, \\ z(\cdot, t) &= 0 & \text{in } \partial\omega \times (0, t_e), \end{aligned}$$

where  $\omega = (a, b) \subset \mathbb{R}$  is an open interval,  $z : \omega \times [0, t_e] \rightarrow \mathbb{R}$  denotes the state, and the parameters  $\varepsilon$ ,  $\gamma$ , and  $\mu$  are real positive constants. The controls are elements of the closed, convex, bounded set  $U_{\text{ad}} = \{u \in L^2(0, t_e; \mathbb{R}) \mid u(t) \in U_{\text{ad}} \text{ for } t \geq 0\}$  with  $U_{\text{ad}} = \{u \in \mathbb{R} \mid u_a \leq u \leq u_b\}$ , with given  $u_a, u_b \in \mathbb{R}$ . Later, we will consider  $U_{\text{ad}}$  as a discrete set in the approximation of the HJB equation. The initial value and the shape function are denoted, respectively, by  $z_o$  and  $b$ . Note that we deal with zero Dirichlet boundary conditions. Let us mention that (6.1) includes the linear heat equation ( $\mu = 0, \gamma = 0$ ), linear advection diffusion equation ( $\mu = 0$ ), and a semilinear parabolic problem with a reaction term ( $\gamma \neq 0, \mu \neq 0$ ). As explained in the previous section, we need to choose  $t_e$  big enough to have an accurate approximation of the infinite horizon problem.

The cost functional we want to minimize is given by

$$(6.2) \quad \widehat{J}(u; z_o) = \int_0^{t_e} \left( \|z(\cdot, t; u) - \bar{z}\|_{L^2(\omega)}^2 + \alpha |u(t)|^2 \right) e^{-\lambda t} dt,$$

where  $z(\cdot, t; u)$  is the solution to (6.1) at time  $t$ ,  $\bar{z}$  is the desired state,  $\alpha \in \mathbb{R}^+$  holds, and  $\lambda > 0$  is the discount factor. The optimal control problem can be formulated as

$$(6.3) \quad \min \widehat{J}(u; z_o) \quad \text{such that } u \in U_{\text{ad}}.$$

We spatially discretize the state equation (6.1) by the standard finite difference method. This approximation leads to the following semidiscrete system of ODEs:

$$(6.4) \quad \begin{aligned} My_t - \varepsilon Ay + \gamma Hy + \mu F(y) &= Bu & \text{in } (0, t_e], \\ y(0) &= y_o, \end{aligned}$$

where  $y : [0, t_e] \rightarrow \mathbb{R}^n$  is an approximation for the solution  $z(\cdot, t)$  to (6.1) at  $n$  spatial grid points,  $A, H \in \mathbb{R}^{n \times n}$ ,  $B, y_o \in \mathbb{R}^n$ , and  $F : \mathbb{R}^n \rightarrow \mathbb{R}^n$  is given by

$$F(y) = \begin{pmatrix} y_1 - y_1^3 \\ \vdots \\ y_n - y_n^3 \end{pmatrix} \quad \text{for } y = (y_1, \dots, y_n) \in \mathbb{R}^n.$$

Here, we do not consider Assumption 2.1 for our underlying problem. Let us mention that problem (6.3) has been already investigated. For instance, existence and uniqueness results for (6.3) can be found in [7]. In general, the dimension  $n$  of the dynamical system (6.4) is rather large (i.e.,  $n \gg 10$ ), so that we cannot solve the HJB equations numerically. Therefore, we apply the POD method in order to reduce the dimension of the optimal control problem and solve it by HJB equations. That fits into our problem  $(\widehat{\mathbf{P}})$ , and therefore we can apply Algorithm 5.1 to solve our optimal control problem.

In the next subsections we will present our numerical tests; in particular we draw our attention on the estimate presented in Theorem 4.8. Although the estimate is not practical since it is unfeasible to compute the true value function, it helps us

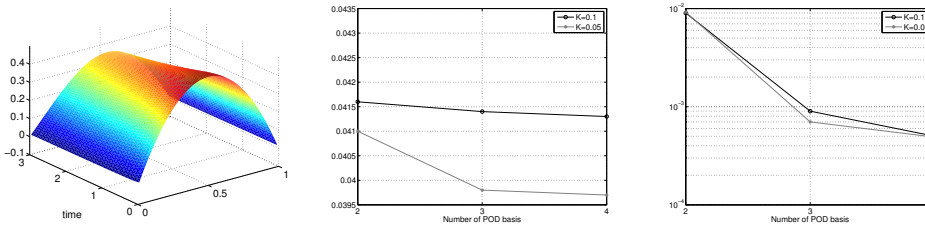


FIG. 6.1. Test 1: Uncontrolled solution (left), evaluation of the cost functional (middle), and distance between  $y(u^\ell)$  and  $y^\ell(u^\ell)$  (right).

choose the parameters  $h, K, \ell$ . In particular, the number of basis functions can be selected as explained in section 5. In order to check the quality of the suboptimal solution, it is hard to find an analytical representation of the value function. However, a particular case is the so-called linear quadratic regulator (LQR) problem, where the dynamics is linear and the cost functional is quadratic. Under these particular conditions we are able to compute the error of our approximation of the value function. Furthermore, for a nonlinear problem, the quality of the computed suboptimal control  $u^\ell$  we will be plugged into the full model  $y(u^\ell)$  and into the surrogate model  $y^\ell(u^\ell)$ , and we can evaluate the cost functional. We note that the nonlinear example discussed above is not stable in open-loop, as mentioned in [7, 8]; therefore feedback control is mandatory to ensure stabilization of the problem. Furthermore, in section 6.3, we test our problem under perturbation of the state to show the robustness of the method. For the sake of completeness we also mention that other model order reduction methods have been combined with the HJB approach. We refer to [6] for a comparison.

**6.1. Test 1: Semilinear equation.** Our first test concerns the semilinear equation. In (6.1) we set  $t_e = 3, \varepsilon = 0.1, \gamma = 0, \mu = 1, \omega = (0, 1)$ , and  $z_o(x) = 2(x - x^2)$ . The shape function  $b$  is equal to the initial condition  $z_o$ . In (6.2) we choose  $\lambda = 1$  and  $\bar{z} = 0$ . To compute the POD basis we determine solutions to the state equation for controls in the set  $U_{\text{snap}} = \{-1, 0, 1\}$  with a semi-implicit finite difference scheme with time step of 0.05 and space step of 0.01. In (4.15) we consider  $K \in \{0.1, 0.05\}, h = 0.1K$ . The optimal trajectory is obtained with a time step size of 0.05. The control set  $\mathbb{U}_{\text{ad}}$  is given by 21 controls equally distributed in  $[-1, 1]$ . In this test we have chosen the following domain for reduced coordinates:  $\Omega^\ell = [-17.4, 7.8] \times [-0.7, 0.7] \times [-0.1, 0.1] \times [-0.1, 0.1]$ . We verified that, in this situation, the strong invariance condition

$$(6.5) \quad y^\ell + hf^\ell(y^\ell, u) \in \Omega^\ell \quad \text{for all } y^\ell \in \Omega^\ell \text{ and } u \in \mathbb{U}_{\text{ad}}$$

holds true.

The uncontrolled solution is shown on the left of Figure 6.1. As we can see, the semilinear part does not allow us to stabilize the solution to zero; our goal is to steer the solution to the origin. The optimal solution and its correspondent optimal controls are shown in Figure 6.2. Moreover, we plot the differences between the computed solutions (please note the different scaling of the pictures). As we can see, the difference decreases when the number of POD basis functions increases. The quality of our approximation is confirmed by Figure 6.1. In the middle panel we plot the decay of the cost functional  $\hat{J}(u^\ell, \omega_o)$ , whereas the distance between  $y(u^\ell)$  and  $y^\ell(u^\ell)$  is plotted in the right panel of Figure 6.1. As expected, the cost functional

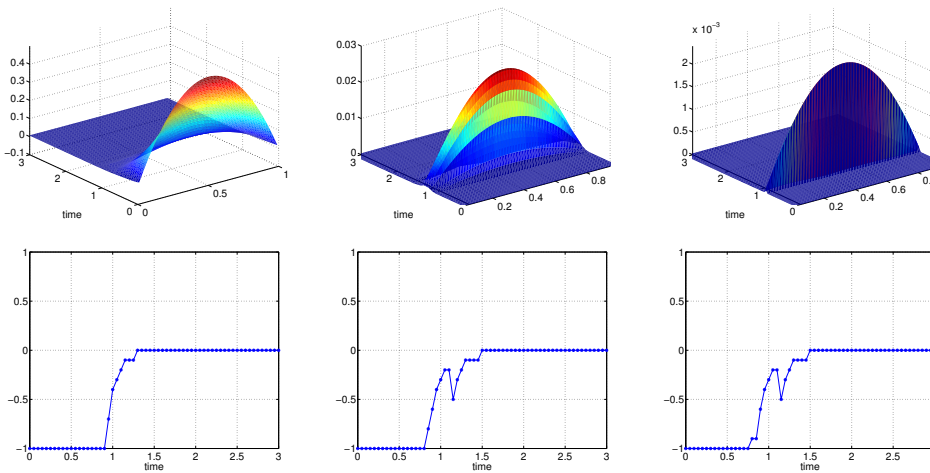


FIG. 6.2. *Test 1: Optimal HJB states computed with Algorithm 5.1 with  $\ell = 4$  POD basis functions (top-left), difference between optimal solution with 4 POD basis and 2 POD basis (top-middle), difference between optimal solution with 4 POD basis and 3 POD basis (top-right), optimal HJB controls with  $\ell = 2, 3, 4$  (bottom).*

and the error in the state decrease when  $\ell$  increases and  $K$  decreases. In this case the error decays much faster than in the previous example. This depends on the decay of the singular value of the snapshots set, as shown in Figure 6.6 below.

**6.2. Test 2: Advection-diffusion equation.** The second test concerns the linear advection-diffusion equation; in (6.1) we set  $t_e = 3$ ,  $\varepsilon = 0.1$ ,  $\gamma = 1$ ,  $\mu = 0$ ,  $\omega = (0, 2)$ , and  $z_o(x) = 0.5 \sin(\pi x)$ . The shape function  $b$  is the characteristic function over the subset  $(0.5, 1) \subset \omega$ . In (6.2) we choose  $\lambda = 1$  and  $\bar{z} = 0$ . To compute the POD basis we determine solutions to the state equation for the following discrete set of controls:  $U_{\text{snap}} = \{-2.2, -1.1, 0\}$ . In (4.15) we consider  $K \in \{0.1, 0.05\}$ ,  $h = 0.1K$ , and the optimal trajectory is obtained with a time step size of 0.05 for the implicit Euler method. The control set  $\mathbb{U}_{\text{ad}}$  is given by 23 controls equally distributed in  $[-2.3, 0]$ . In this test we have chosen the following domain for reduced coordinates:  $\Omega^\ell = [-2.5, 2.5] \times [-2, 2] \times [-1.5, 1.5] \times [-1, 1]$ . We note that, although the strong invariance condition (6.5) is not satisfied, a weaker condition holds true, namely,

$$(6.6) \quad \text{for all } y^\ell \in \Omega^\ell \text{ there exists } u \in \mathbb{U}_{\text{ad}} : y^\ell + h f^\ell(y^\ell, u) \in \text{int}(\Omega^\ell),$$

where  $\text{int}(\Omega^\ell)$  denotes the interior of  $\Omega^\ell$ . It is interesting to note that, reducing the control space to the controls in  $\mathbb{U}_{\text{ad}}$  which satisfy condition (6.6), our code is able to compute a value function with rather accurate results comparable with those obtained via the LQR approach. Thus, the condition seems to be sufficient to set up the proposed approximation, although this situation is not covered by the theorem. A more detailed analysis of problems with state constraints will be addressed in the near future. In Figure 6.3(left) we show the solution of the uncontrolled (6.1), i.e., for  $u \equiv 0$ . Since our problem is linear-quadratic, the solution of the HJB equation can be computed by solving the well-known Riccati equation (for the LQR approach, see [16]). Then, the optimal LQR state is as presented in Figure 6.3(middle), whereas the optimal LQR control is as plotted in Figure 6.3(right).

We show the controlled solution computed by means of Algorithm 5.1 on the left of Figure 6.4. Since it is hard to visualize differences from the optimal solutions, we

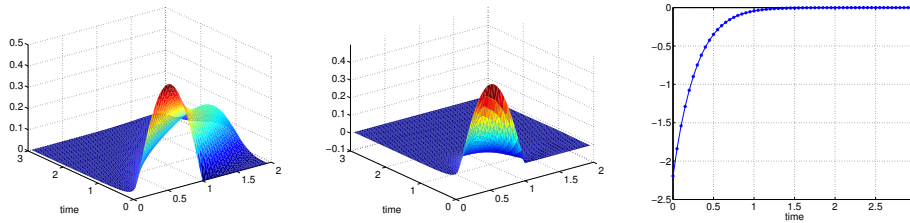


FIG. 6.3. Test 2: Uncontrolled solution (left), LQR optimal solution (middle), LQR optimal control (right).

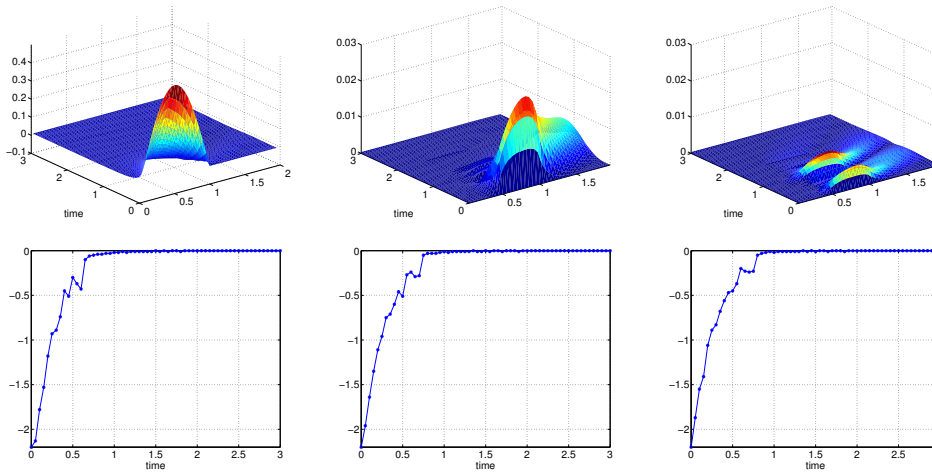


FIG. 6.4. Test 2: Optimal HJB states computed with Algorithm 5.1 with  $\ell = 4$  POD basis functions (top-left), difference between optimal solution with 4 POD basis and 2 POD basis (top-middle), difference between optimal solution with 4 POD basis and 3 POD basis (top-right), optimal HJB controls with  $\ell = 2, 3, 4$  (bottom).

plot the difference between the optimal solution obtained with 4 POD basis functions and that obtained with 2 (middle) or 3 (right) POD basis functions. In order to analyze our numerical approximation we consider the evaluation of the cost functional  $\widehat{J}(u^\ell; y_o)$ , the distance between  $y(u^\ell)$  and  $y^\ell(u^\ell)$ , and the error between the true LQR solution and the suboptimal  $y(u^\ell)$ . The error analysis is shown in Figure 6.5. On the left we show the decay of the cost functional when we increase the number of POD basis functions. In the middle we compute the  $L^2$ -error between the optimal reduced solution  $y^\ell(u^\ell)$  and the suboptimal solution  $y(u^\ell)$ . Even in this case the error decays when  $\ell$  increases and  $K$  decreases. This error measures the quality of the surrogate model, since we want to check whether the suboptimal control fits into the nonreduced problem. Finally, on the right, we compute the error between the optimal solution and the suboptimal  $y(u^\ell)$ . As expected, increasing the number of basis function and decreasing the step size  $K$  (remember that  $h$  and  $K$  are linked) for the approximation of the value function, the optimal solution is improved.

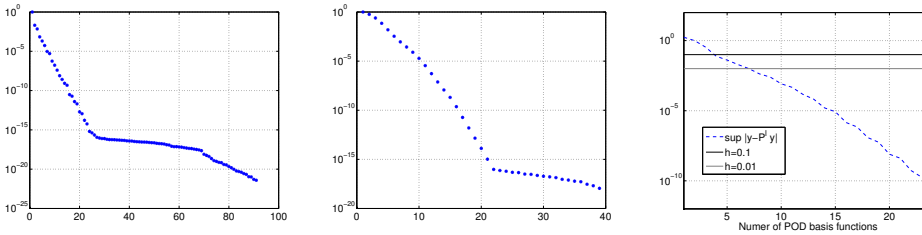


FIG. 6.6. Decay of the singular values for the snapshots set associated with Test 1 (left) and Test 2 (middle). Plot of term  $\sup_{y \in \overline{\Omega}} \|y - \mathcal{P}^\ell y\|_2$  in (4.24) (right).

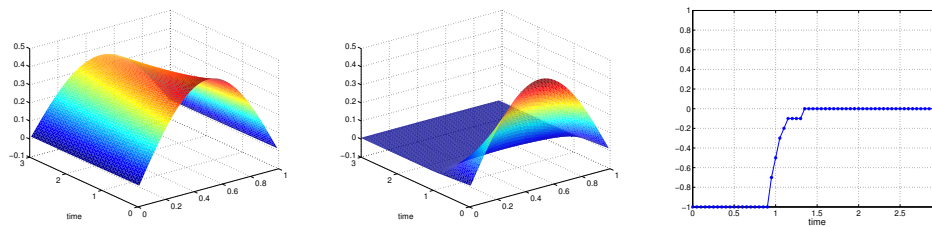


FIG. 6.7. Test 3: Uncontrolled solution (left), optimal state (middle), and corresponding optimal HJB control (right).

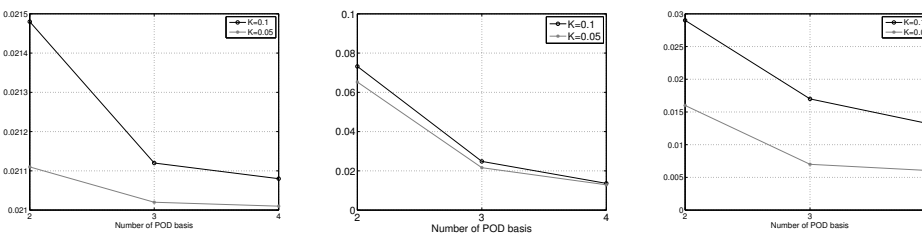


FIG. 6.5. Test 2: Evaluation of the cost functional (left),  $L^2$ -error for  $y(u^\ell)$  and  $y^\ell(u^\ell)$  (middle), and  $L^2$ -error between LQR solution and  $y(u^\ell)$  (right). The black line refers to the approximation with  $K = 0.1$  in HJB, whereas the gray one to  $K = 0.05$ .

The decay of the singular values is presented in Figure 6.6. Finally, we want to give an idea of the term  $\sup_{y \in \overline{\Omega}} \|y - \mathcal{P}^\ell y\|_2/h$  in the error estimate (4.24). It is clear we do not know  $\Omega$ , but we chose several random control sequences in the set of admissible controls in order to have an approximation of the set. Now, we can compute the aforementioned error term. The decay is shown in Figure 6.6(right). This term would help us select the number of POD basis functions in order to get an error of order  $o(h)$ , as explained in Remark 4.9.

**6.3. Test 3: Semilinear equation with uniform noise.** In this test we deal with the semilinear equation discussed in Test 1, but we add noise to the optimal trajectory. The uncontrolled solution is shown on the left of Figure 6.7, the optimal trajectory in the middle panel, and the control computed by means of Algorithm 5.1 in the right panel.

The goal is to show the stabilization of the feedback control under strong perturba-

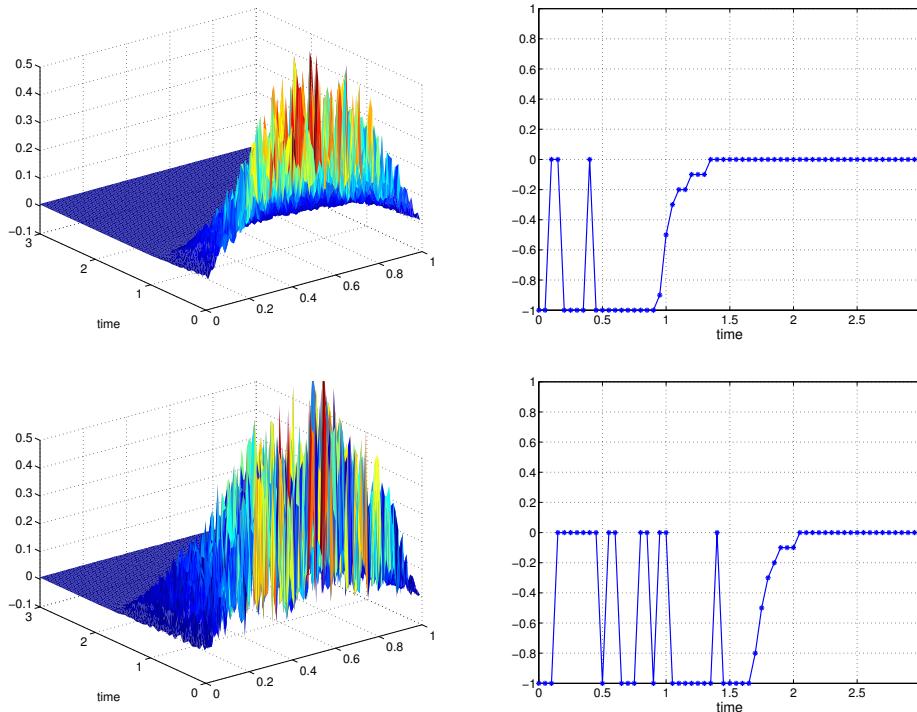


FIG. 6.8. *Test 3: Optimal HJB-POD state (left) and corresponding optimal control (right) with  $|\eta(x)| \leq 50\%$  (top) and  $|\eta(x)| \leq 90\%$  noise (bottom).*

tions of the system. We note that in this case the value function is stored from the system without perturbation, but the reconstruction of the feedback control is affected by uniform noise  $\eta(x)$  in the interval  $[-1, 1]$  in every time step:  $y(x, \cdot) = (1 + \eta(x))y(x, \cdot)$ . Figure 6.8 shows the optimal solution and control corresponding to different noise levels. In this example we can see the power of the feedback control and, in particular, the importance of the knowledge of the value function. In both examples, the trajectory is stabilized close to the origin. If we look at the optimal control input, we can observe a strong chattering. In both cases the optimal control jumps often from  $-1$  to  $0$ . In particular, in the second case, it is possible to observe stronger chattering due to the high disturbances. Nevertheless, the feedback control is able to stabilize the perturbed system.

**7. Conclusion and remarks.** In this paper we present a new a priori error analysis for the coupling between the HJB equation and the POD method. The proposed estimate is presented for infinite horizon control problems with linear and nonlinear dynamical systems, but this approach could be also applied to other optimal control problems, provided one has a priori estimates on the approximation based on the HJB equation. The convergence of the method is guaranteed under rather general assumptions on the optimal control problem and some technical assumptions on the dynamics and on the POD approximation. For the latter, it is clear that a clever choice of the snapshots set can play a crucial role in the estimate in reducing the contribution of the POD approximation in the a priori estimate. Several choices are possible based on greedy techniques or on a previous open-loop approximation;

these choices will be investigated in a future paper. At present, the numerical tests illustrated in the last section confirm our theoretical findings and show the robustness of the Bellman approach also under strong disturbances of the dynamical system.

## REFERENCES

- [1] A. ALLA AND M. FALCONE, *An adaptive POD approximation method for the control of advection-diffusion equations*, in Control and Optimization with PDE Constraints, K. Kunisch, K. Bredies, C. Clason, and G. von Winckel, eds., Internat. Ser. Numer. Math. 164, Birkhäuser, Basel, 2013, pp. 1–17.
- [2] A. ALLA, M. FALCONE, AND D. KALISE, *An efficient policy iteration algorithm for dynamic programming equations*, SIAM J. Sci. Comput., 37 (2015), pp. A181–A200, <https://doi.org/10.1137/130932284>.
- [3] A. ALLA AND M. HINZE, *HJB-POD feedback control for Navier-Stokes equations*, in Proceedings of the 18th European Conference on Mathematics for Industry (ECMI), Springer, 2014, pp. 861–868.
- [4] A. ALLA AND M. HINZE, *HJB-POD feedback control of advection-diffusion equation with a model predictive control snapshot sampling*, IFAC-PapersOnLine, 48 (2015), pp. 527–532.
- [5] J.A. ATWELL AND B.B. KING, *Proper orthogonal decomposition for reduced basis feedback controllers for parabolic equations*, Math. Comput. Modelling, 33 (2001), pp. 1–19.
- [6] A. ALLA, A. SCHMIDT, AND B. HAASDONK, *Model order reduction approaches for infinite horizon optimal control problems via the HJB equation*, Model Reduction of Parametrized Systems III (Proceedings of MoRePas III), 2017, Chapter 21.
- [7] A. ALLA AND S. VOLKWEIN, *Asymptotic stability and suboptimality of model predictive control for semilinear PDEs*, Adv. Comput. Math., 41 (2015), pp. 1073–1102.
- [8] N. ALTMÜLCER, L. GRÜNE, AND K. WORTHMANN, *Receding horizon optimal control for the wave equation*, in Proceedings of the 49th IEEE Conference on Decision and Control, 2010, pp. 3427–3432.
- [9] M. BARDI AND I. CAPUZZO-DOLCETTA, *Optimal Control and Viscosity Solutions of Hamilton-Jacobi-Bellman Equations*, Birkhäuser, Basel, 1997.
- [10] M. BARRAULT, Y. MADAY, N.C. NGUYEN, AND A.T. PATERA, *An “empirical interpolation” method: Application to efficient reduced-basis discretization of partial differential equations*, C.R. Math., 339 (2004), pp. 667–672.
- [11] P. BENNER, S. SACHS, AND S. VOLKWEIN, *Model order reduction for PDE constrained optimization*, in Trends PDE Constrained Optimization, Internat. Ser. Numer. Math. 165, Birkhäuser, 2014, pp. 303–326.
- [12] S. CACACE, E. CRISTIANI, M. FALCONE, AND A. PICARELLI, *A patchy dynamic programming scheme for a class of Hamilton–Jacobi–Bellman equations*, SIAM J. Sci. Comput., 34 (2012), pp. A2625–A2649, <https://doi.org/10.1137/110841576>.
- [13] F. CAMILLI, M. FALCONE, P. LANUCARA, AND A. SEGHINI, *A domain decomposition method for Bellman equations*, in Domain Decomposition Methods in Scientific and Engineering Computing, D. E. Keyes and J. Xu, eds., Contemp. Math. 180, AMS, 1994, pp. 477–483.
- [14] D. CHAPPELLE, A. GARIAH, AND J. SAINT-MARIE, *Galerkin approximation with proper orthogonal decomposition: New error estimates and illustrative examples*, ESAIM: Math. Model. Numer. Anal., 46 (2012), pp. 731–757.
- [15] S. CHATURANTABUT AND D.C. SORENSEN, *Nonlinear model reduction via discrete empirical interpolation*, SIAM J. Sci. Comput., 32 (2010), pp. 2737–2764, <https://doi.org/10.1137/090766498>.
- [16] R.F. CURTAIN AND H.J. ZWART, *An Introduction to Infinite-Dimensional Linear Systems Theory*, Springer, 1995.
- [17] M. FALCONE, *A numerical approach to the infinite horizon problem of deterministic control theory*, Appl. Math. Optim., 15 (1987), pp. 1–13.
- [18] M. FALCONE, *Numerical solution of dynamic programming equations*, in Optimal Control and Viscosity Solutions of Hamilton–Jacobi–Bellman Equations, Birkhäuser, Basel, 1997, pp. 471–531.
- [19] M. FALCONE AND R. FERRETTI, *Semi-Lagrangian Approximation Schemes for Linear and Hamilton–Jacobi Equations*, SIAM, Philadelphia, 2014.
- [20] M. FALCONE AND T. GIORGI, *An approximation scheme for evolutive Hamilton–Jacobi equations*, in Stochastic Analysis, Control, Optimization and Applications: A Volume in Honor of W.H. Fleming, W.M. McEneaney, G. Yin, and Q. Zhang, eds., Birkhäuser, Boston, 1999, pp. 289–303.



- [21] M. FALCONE, P. LANUCARA, AND A. SEGHINI, *A splitting algorithm for Hamilton-Jacobi-Bellman equations*, Appl. Numer. Math., 15 (1994), pp. 207–218.
- [22] W.H. FLEMING AND H.M. SONER, *Controlled Markov Processes and Viscosity Solutions*, Springer-Verlag, New York, 1993.
- [23] J. GARCKE AND A. KRÖNER, *Suboptimal feedback control of PDEs by solving HJB equations on adaptive sparse grids*, J. Sci. Comput., 70 (2017), pp. 1–28.
- [24] R. GLOWINSKI, J.L. LIONS, AND R. TRÉMOLIÈRES, *Analyse Numerique des Inéquations Variationnelles*, Dunod-Bordas, Paris, 1976.
- [25] M. GUBISCH AND S. VOLKWEIN, *Proper orthogonal decomposition for linear-quadratic optimal control*, in Model Reduction and Approximation: Theory and Algorithms, P. Benner, A. Cohen, M. Ohlberger, and K. Willcox, eds., Comput. Sci. Eng. 15, SIAM, Philadelphia, 2017, pp. 3–64.
- [26] P. HOLMES, J.L. LUMLEY, G. BERKOOZ, AND C.W. ROWLEY, *Turbulence, Coherent Structures, Dynamical Systems and Symmetry*, 2nd ed., Cambridge Monogr. Mech., Cambridge University Press, 2012.
- [27] M. HINZE, R. PINNAU, M. ULBRICH, AND S. ULBRICH, *Optimization with PDE Constraints*, Math. Model. Theory Appl. 23, Springer-Verlag, 2009.
- [28] M. HINZE AND S. VOLKWEIN, *Proper orthogonal decomposition surrogate models for nonlinear dynamical systems: Error estimates and suboptimal control*, in Reduction of Large-Scale Systems, P. Benner, V. Mehrmann, and D.C. Sorensen, eds., Lecture Notes Comput. Sci. Engrg. 45, 2005, pp. 261–306.
- [29] D. KALISE AND A. KRÖNER, *Reduced-order minimum time control of advection-reaction-diffusion systems via dynamic programming*, in Proceedings of the 21st International Symposium on Mathematical Theory of Networks and Systems, 2014, pp. 1196–1202.
- [30] A. KRÖNER, K. KUNISCH, AND H. ZIDANI, *Optimal feedback control for undamped wave equations by solving a HJB equation*, ESAIM Control Optim. Calc. Var., 21 (2015), pp. 442–464.
- [31] K. KUNISCH, S. VOLKWEIN, AND L. XIE, *HJB-POD based feedback design for the optimal control of evolution problems*, SIAM J. Appl. Dyn. Syst., 4 (2004), pp. 701–722, <https://doi.org/10.1137/030600485>.
- [32] K. KUNISCH AND L. XIE, *POD-based feedback control of Burgers equation by solving the evolutionary HJB equation*, Comput. Math. Appl., 49 (2005), pp. 1113–1126.
- [33] F. LEIBFRITZ AND S. VOLKWEIN, *Reduced order output feedback control design for PDE systems using proper orthogonal decomposition and nonlinear semidefinite programming*, Linear Algebra Appl., 415 (2006), pp. 542–575.
- [34] C. NAVASCA AND A.J. KRENER, *Patchy solutions of Hamilton-Jacobi-Bellman partial differential equations*, in Modeling, Estimation and Control, Lecture Notes in Control and Inform. Sci. 364, Springer, New York, 2007, pp. 251–270.
- [35] A. QUARTERONI AND A. VALLI, *Domain Decomposition Methods for Partial Differential Equations*, Oxford University Press, London, 1999.
- [36] A. QUARTERONI, A. MANZONI, AND F. NEGRI, *Reduced Basis Methods for Partial Differential Equations*, Springer-Verlag, Berlin, 2016.
- [37] J.A. SETHIAN, *Level Set Methods and Fast Marching Methods*, Cambridge University Press, 1999.
- [38] J.A. SETHIAN AND A. VLADIMIRSKY, *Ordered upwind methods for static Hamilton-Jacobi equations: Theory and algorithms*, SIAM J. Numer. Anal., 41 (2003), pp. 325–363, <https://doi.org/10.1137/S0036142901392742>.
- [39] J.R. SINGLER, *New POD expressions, error bounds, and asymptotic results for reduced order models of parabolic PDEs*, SIAM J. Numer. Anal., 52 (2014), pp. 852–876, <https://doi.org/10.1137/120886947>.
- [40] H.M. SONER, *Optimal control with state-space constraint. I*, SIAM J. Control Optim., 24 (1986), pp. 552–561, <https://doi.org/10.1137/0324032>.
- [41] H.M. SONER, *Optimal control with state-space constraint. II*, SIAM J. Control Optim., 24 (1986), pp. 1110–1122, <https://doi.org/10.1137/0324067>.
- [42] Y.-H.R. TSAI, L.-T. CHENG, S. OSHER, AND H.-K. ZHAO, *Fast sweeping algorithms for a class of Hamilton-Jacobi equations*, SIAM J. Numer. Anal., 41 (2003), pp. 673–694, <https://doi.org/10.1137/S0036142901396533>.
- [43] F. TRÖLTZSCH, *Optimal Control of Partial Differential Equations: Theory, Methods and Application*, AMS, Providence, RI, 2010.